TECHNICAL REPORT R-10

STAGNATION-POINT SHIELDING BY MELTING AND VAPORIZATION

By LEONARD ROBERTS

Langley Research Center
Langley Field, Va.

TECHNICAL REPORT R-10

STAGNATION-POINT SHIELDING BY MELTING AND VAPORIZATION

By Leonard Roberts

SUMMARY

A theoretical study is made of the shielding mechanism whereby the rates of heat transfer are reduced near the stagnation point of two-dimensional and three-dimensional bodies when melting and vaporization occur simultaneously. The problem is approximated to its simplest form consistent with the mass-transfer and heat-transfer conditions. Simple results are presented which give the rate of mass loss at the body surface and the thickness of the liquid layer at the surface in terms of the rate of heat transfer to the unshielded body.

INTRODUCTION

The shielding of the nose of a body from excessive rates of heat transfer by melting or vaporization has been shown to be particularly attractive in view of the proportion of heat convected away from the nose in the boundary layer. (See refs. 1 to 4.)

The extent of the shielding depends on the rate of mass loss, the manner in which the mass is removed, and its thermal capacity. Thus, it may be expected that the properties of the material in its molten and gaseous states, as well as in the solid state, play an important part in determining its suitability as an ablation shield. Since the rate of mass loss depends on the rate of heat transfer to the surface, the choice of material is very important inasmuch as this is the only control on the ablation rate left to the designer.

Theoretical studies of surface melting have been made previously (refs. 1 and 2) where the convection of heat by the molten material provides some shielding. When vaporization of the liquid is not considered, this shielding is necessarily limited to the heat convected by the liquid. When vaporization of the liquid is considered, however, the shielding can increase considerably because of the latent heat of vaporization and because the gaseous products now diffuse to the regions of higher (stagnation) temperature and are convected in those regions (refs. 4 and 5). Whereas it is probably more desirable to have direct vaporization without a liquid film (since this precludes possible instabilities in the liquid film), it may be more efficient from overall heat-capacity considerations to have a material which, during ablation, produces both liquid and gaseous layers near the surface.

This situation is considered in the present report by an extension of the simple analyses made in references 4 and 5. An important feature of this more general type of ablation is the interaction of the gas and liquid layers due to vaporization at the gas-liquid interface. This interaction plays an important part in determining the proportion of total ablated mass which is vaporized. Ablation with no vaporization of the liquid layer is obtained as a special case of this more general treatment.

SYMBOLS

x	coordinate along solid surface
y	coordinate normal to solid surface with origin at solid surface
y'	coordinate normal to solid surface with origin at interface
z	transformed y-coordinate
Z	arbitrary value of z outside gas boundary layer
u	component of velocity in x-direction
v	component of velocity in y-direction

U	free-stream velocity in x-direction
C	constant in velocity distribution
C_l	constant in velocity distribution for liquid
T	temperature
W	mass concentration of foreign gas
$\overline{W}$	effective mean concentration
p	pressure
p_o	pressure at stagnation point
ρ	density
μ	coefficient of viscosity
k	thermal conductivity
D_{12}	coefficient of binary diffusivity
$\dot{m}$	total rate of mass loss per unit area of wall
$\dot{m}_i$	rate of vaporization per unit area of interface
c_p	specific heat at constant pressure
$\overline{c}_p$	mean effective specific heat of gas mixture
c_l	specific heat of liquid
c_b	specific heat of solid
L_m	latent heat of melting
L_v	latent heat of vaporization
$\frac{n_1}{n_1+n_2}, \frac{n_2}{n_1+n_2}$	fractions of gas and air in 1 mole of mixture
M	molecular weight
R	gas constant
Su	constant in Sutherland viscosity law
N_{Nu}	Nusselt number, $\frac{x}{T_e-T_i}\frac{dT}{dy}$
R_i	Reynolds number at interface, $\frac{C\rho_i}{\mu_i}x^2$
N_{Sc}	Schmidt number, $\frac{\mu}{\rho D_{12}}$
N_{Pr}	Prandtl number, $\frac{\mu}{k}c_{p,2}$
C_f	skin-friction coefficient
τ	shear stress
q	rate of heat transfer per unit area
δ	physical boundary-layer thickness
δ_u	transformed velocity-boundary-layer thickness
δ_T	transformed thermal-boundary-layer thickness
δ_W	transformed concentration-boundary-layer thickness
Δ_m	momentum thickness of gas boundary layer
Δ^*	displacement thickness of gas boundary layer
D	liquid-layer thickness
θ	thermal-layer thickness within solid
Q_0, Q_1, Q_2, Q_3	enthalpy parameters (defined by eqs. (60a), (60d), (60e), and (60f), respectively)
J	additional effect due to boiling (eq. 29(b))
$\alpha_1, \alpha_2, \alpha_3, \alpha_4$	functions of $\frac{\rho_e\mu_e}{\rho_i\mu_i}$ (defined by eqs. (60), (63), (64), and (68) or (69))
H_{eff}	effective heat capacity (eq. (82))
Subscripts:	
e	external flow near stagnation point
i	gas-liquid interface
w	wall
b	body
l	liquid
0	no ablation
B	value at boiling point of liquid
1	foreign gas
2	air
max	maximum
2-dim	two-dimensional
A	axisymmetric

THE SHIELDING MECHANISM

The flow configuration considered is shown in figure 1. The coordinate system is fixed in the melting surface at the stagnation point so that the interior of the body moves with velocity v_b, the ablation rate, toward the surface. In the steady state there is a balance within the solid of conductive and convective heat transfer (due to the motion of the solid).

For sufficiently high rates of heat transfer a liquid film is produced by melting, the motion of which is controlled by the pressure gradient imposed by the outside stream and the shear stress at the interface. It is shown that, when no vaporization occurs, the presence of the liquid film has negligible effect on the air-boundary-layer flow so that the interface shear stress assumes the value that holds in the presence of a fixed boundary.

As the rate of heat transfer increases, the thickness of the liquid layer changes until the interface

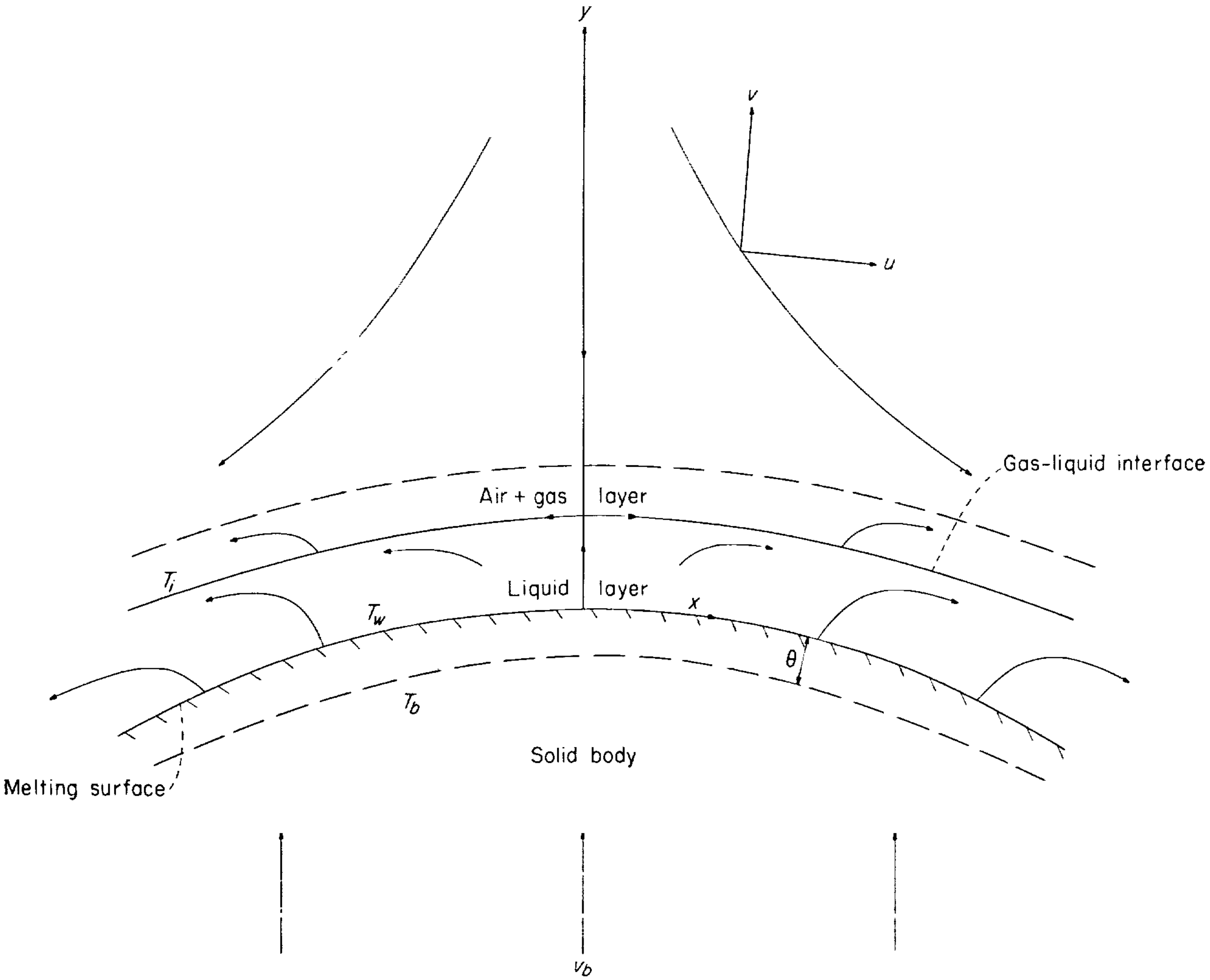

FIGURE 1.—Flow configuration.

forces are in balance; the interface temperature increases to such a value that the convective shielding by the liquid layer is compatible with the rate of heat transfer at the surface required to produce the liquid. As the heat-transfer rate increases further, the rate of vaporization becomes sufficiently large to affect the character of the air boundary layer. This has two important effects on the interface conditions: Firstly, the rate of heat transfer across the interface is partly reduced because of shielding by the gas products and, secondly, the introduction of gas at the interface reduces the interface skin friction. As a result of this second effect the liquid layer tends to become thicker with an attendant reduction of gradients at the wall, although this trend is somewhat diminished and even reversed because the viscosity of the liquid decreases as the temperature increases. For a given rate of vaporization it is shown that the motion of the liquid film has a negligible effect on the gas boundary layer.

In the gas boundary layer the gas produced by vaporization diffuses away from the interface and is convected as a mixture (of air and gas) parallel to the body surface. For exteme heating rates this convection can make the major contribution to the total shielding, since the gas is raised to the higher temperatures. This particular phase of shielding has been investigated in reference 4.

Thus, it is seen that the ablation rate is controlled by the net heat transfer to the wall; this heat transfer, however, is itself greatly influenced by the manner in which the products of ablation are removed from the wall. The analysis explains in a more precise fashion the balance of heat transfer and mass transfer which produces this shielding phenomenon.

ANALYSIS

HEAT TRANSFER IN THE SOLID

For a solid moving with constant velocity v_b toward the surface $y=0$, the transfer of heat is governed approximately by the following equation:

$$\underbrace{\frac{d}{dy}\left(k_b\frac{dT}{dy}\right)}_{\substack{\text{Diffusion of heat}\\ \text{to interior}}} = \underbrace{\dot{m}c_b\frac{dT}{dy}}_{\substack{\text{Convection of heat}\\ \text{toward surface}}} \qquad (1)$$

Equation (1) neglects temperature gradients parallel to the surface and is therefore a good approximation when the thickness of the solid ablation shield is large compared with the thickness of the thermal layer θ within the solid (near the surface) in which the temperature changes rapidly from its value at the wall T_w (the melting temperature) to its value at the far interior T_b. (See fig. 1.)

Equation (1) has the solution

$$T=T_b+(T_w-T_b)e^{\frac{\dot{m}c_b y}{k_b}} \qquad (2)$$

which satisfies the condition $T=T_w$ at $y=0$ and the condition $T=T_b$ as $y\rightarrow-\infty$ (with T_w and T_b constant).

The thickness of the thermal layer near the surface is defined as follows:

$$\theta=\int_{-\infty}^{0}\frac{T-T_b}{T_w-T_b}\,dy=\frac{k_b}{\dot{m}c_b} \qquad (3)$$

In order to confine the high temperatures to a thin region near the surface, it is desirable to have a material of low conductivity k_b and high specific heat c_b.

The rate of heat transfer away from the surface toward the interior at $y=0$ is obtained from equation (2) and is written

$$\left(k_b\frac{dT}{dy}\right)_{w-}=c_b(T_w-T_b)\dot{m} \qquad (4)$$

where the subscript $w-$ denotes that the surface is approached through negative values of y. The rate of mass loss $\dot{m}$ is unknown at this stage and must be determined by consideration of the liquid layer and the gas boundary layer.

THE BOUNDARY CONDITIONS

The method employed in the following sections assumes that the detailed variation of the velocity, temperature, and concentration profiles is of secondary importance so that they may be approximated in the simplest manner. It is important, however, that the boundary conditions which describe the transfer of heat and mass at the melting surface and at the gas-liquid interface be carefully formulated and respected.

Melting conditions.—The heat-transfer condition at the wall is

$$\underbrace{\left(k\frac{dT}{dy}\right)_w}_{\substack{\text{Heat transfer}\\ \text{to wall}}} = \underbrace{L_m\dot{m}}_{\substack{\text{Latent heat}\\ \text{of melting}}} + \underbrace{c_b(T_w-T_b)\dot{m}}_{\text{Body heat}} \qquad (5)$$

The last term of equation (5) is given by equation (4) and is the heat required to raise the mass $\dot{m}$ to the temperature T_w, in unit time, before melting.

The mass-transfer condition is

$$\underbrace{\rho_b v_b}_{\text{Solid lost}} = \underbrace{\rho_l v_{l,w}}_{\text{Liquid produced}}=\dot{m} \qquad (6)$$

from which the ablation rate v_b is found when the rate of mass loss is known.

A third condition is that which states that the liquid produced has no component of velocity along the wall, since at the wall the heat transfer, and therefore the melting, takes place along lines normal to the wall; thus

$$u_{l,w}=0 \qquad (7)$$

Finally,

$$T=T_w=\text{Constant} \qquad (8)$$

reflects the assumption that the melting temperature T_w is constant along the wall.

Gas-liquid interface conditions.—The rate of heat transfer through the gas-liquid interface and the skin friction at the interface control the rate of melting at the wall and the manner in which the liquid is removed. These interface values, however, are themselves influenced by the rate of mass transfer across the interface and careful consideration of the boundary conditions is necessary.

It is first shown that the motion of the liquid parallel to the wall has negligible effect on the gas boundary layer in general and on the interface values of skin friction and heat transfer in particular.

The pressure distribution imposed by the outside stream is

$$p_o-p=\frac{1}{2}\rho_e U^2=\frac{1}{2}\rho_e C^2x^2 \tag{9}$$

and the pressure in the liquid at the interface satisfies the relation

$$p_o-p\geqq\frac{1}{2}\rho_l u_{l,i}^2=\frac{1}{2}\rho_l C_l^2x^2 \tag{10}$$

Equation (10) is a statement that the decrease in pressure along the interface away from the stagnation point exceeds the dynamic pressure $\frac{1}{2}\rho_l u_{l,i}^2$ because of the presence of viscous forces; the equality sign holds only when the viscous forces in the liquid layer are negligible.

In order to match the variation with x, equations (9) and (10) require that [1]

$$\frac{1}{2}\rho_e C^2\geqq\frac{1}{2}\rho_l C_l^2 \tag{11}$$

The velocity along the gas-liquid interface is, from equation (11),

$$u_{l,i}=C_l x=\frac{C_l}{C}U\leqq\left(\frac{\rho_e}{\rho_l}\right)^{1/2}U \tag{12}$$

For most liquids the density ratio ρ_e/ρ_l is less than 10^{-4} under the temperature conditions at which ablation can take place; therefore, $u_{l,i}/U<10^{-2}$.

The effect of liquid motion on the interface skin friction is estimated very simply by the following approximations: The shear stress at the interface, for no motion of the liquid, is

$$\left(\mu\frac{\partial u}{\partial y}\right)_i\approx\mu_i\frac{U}{\delta}$$

and, when the interface velocity is $u_{l,i}$, is

$$\left(\mu\frac{\partial u}{\partial y}\right)_i\approx\mu_i\frac{U-u_{l,i}}{\delta}$$

(Here δ is the thickness of the velocity boundary layer in the gas.) The difference in stress expressed as a fraction of the value for no motion of the liquid is $u_{l,i}/U$ and therefore may be neglected.

The effect on the rate of heat transfer across the surface is also easily estimated. The convection of heat in the gas boundary layer parallel to the interface is given by

$$\int_0^\delta \rho c_p(T-T_i)u\,dy'$$

If simple profiles

$$\frac{T-T_i}{T_e-T_i}=\frac{y'}{\delta}$$

$$\frac{u}{U}=\frac{y'}{\delta}$$

are assumed when there is no motion of the liquid layer and an average value of ρc_p is assumed, then the convective heat transfer in the boundary layer parallel to the interface is

$$\frac{1}{3}\delta\rho c_p(T_e-T_i)U$$

When the interface velocity is $u_{l,i}$ and the assumed velocity profile is

$$\frac{u}{U}=\frac{u_{l,i}}{U}+\left(1-\frac{u_{l,i}}{U}\right)\frac{y'}{\delta}$$

then the convective heat transfer is increased to

$$\left(\frac{1}{3}+\frac{1}{6}\frac{u_{l,i}}{U}\right)\delta\rho c_p(T_e-T_i)U$$

The fractional increase is thus $\frac{1}{2}\frac{u_{l,i}}{U}$, that is, it may be neglected, and the corresponding reduction in heat transfer across the interface is negligible.

The interface conditions can now be written without reference to the motion of the liquid. The mass-transfer condition is simply

$$\underset{\text{Liquid lost}}{\rho_l v_{l,i}} \quad = \quad \underset{\text{Gas introduced}}{\rho_i v_i=\dot{m}_i} \tag{13}$$

---

[1] More precisely, it is the normal stress component that should be matched but at the interface this differs from p by a constant so that equation (11) is true exactly.

The heat-transfer condition is

$$\underbrace{\left(k\frac{dT}{dy}\right)_i}_{\substack{\text{Heat transfer}\\ \text{to interface}}} = \underbrace{L_v\dot{m}_i}_{\substack{\text{Latent heat of}\\ \text{vaporization}}} + \underbrace{\left(k\frac{dT}{dy}\right)_{l,i}}_{\substack{\text{Heat transfer away}\\ \text{from interface}}} \tag{14}$$

A third transfer condition is that which states that no air crosses the interface; thus,

$$\underbrace{-\left(\rho D_{12}\frac{dW}{dy}\right)_i}_{\substack{\text{Diffusion of air}\\ \text{toward interface}}} = \underbrace{(1-W_i)\dot{m}_i}_{\substack{\text{Convection of air}\\ \text{away from interface}}} \tag{15}$$

that is, there is a balance of diffusion of air toward the interface and convection of air, of concentration $1-W$, away from the interface.

The concentration of foreign gas also depends on the external pressure and is such that the partial pressure is compatible with the interface temperature. Thus if 1 mole of the binary mixture of air and gas at the interface consists of $\frac{n_1}{n_1+n_2}$ mole of gas and $\frac{n_2}{n_1+n_2}$ mole of air, then the partial pressure of the gas is

$$\frac{p_1}{p_i}=\frac{n_1}{n_1+n_2}$$

and the mass concentration W_i is given by

$$W_i=\frac{n_1M_1}{n_1M_1+n_2M_2}$$

The partial pressure p_1 and the interface temperature are related by the (simplified) Clausius-Clapeyron equation:

$$\frac{p_1}{p_i}=e^{\frac{L_v}{R_1}\left(\frac{1}{T_B}-\frac{1}{T_i}\right)}$$

where T_B is the boiling temperature at the pressure p_i.

Elimination of p_1/p_i and n_1/n_2 from the foregoing equations gives the following relation between W_i and T_i:

$$W_i=\left[1+\frac{M_2}{M_1}\left(e^{\frac{L_v}{R_1}\left(\frac{1}{T_i}-\frac{1}{T_B}\right)}-1\right)\right]^{-1} \tag{16}$$

In addition, there are conditions for the continuity of the components of stress at the interface; that for the normal component has already been given and yields

$$\frac{C_l}{C}\leq\left(\frac{\rho_e}{\rho_l}\right)^{1/2} \tag{17}$$

Continuity of the tangential component of stress gives

$$\left(\mu\frac{\partial u}{\partial y}\right)_i=\left(\mu\frac{\partial u}{\partial y}\right)_{l,i} \tag{18}$$

and, finally, there is no slip along the interface so that

$$u_i=u_{l,i} \tag{19}$$

Equation (19) was tacitly assumed and used to show the negligible effect of liquid motion on the gas layer.

When vaporization occurs, both $\dot{m}_i$ and T_i must be determined as part of the solution. If melting does not occur (that is, when the wall vaporizes directly with no liquid phase), then $\dot{m}=\dot{m}_i$.

The stress condition given by equation (18) is required to determine the magnitude of the liquid velocity $u_{l,i}$ which has an important effect on the liquid-layer shielding (even though it has a negligible effect on the gas layer).

External stream conditions.—It is assumed that the following conditions hold outside the gas boundary layer:

$$\left.\begin{aligned} u&=U=Cx\\ T&=T_e\\ \rho&=\rho_e\\ W&=0 \end{aligned}\right\} \tag{20}$$

These are the usual external conditions for stagnation-point flow; the last condition is a statement that there is no foreign gas outside the boundary layer.

INTERFACE HEAT-TRANSFER AND SKIN-FRICTION RELATIONS

Heat transfer.—Since the motion of the liquid layer has negligible effect on the gas boundary layer, the situation at the interface is exactly that which prevails when a solid surface vaporizes. The heat-transfer and mass-transfer results for such a problem are given in references 4 and 5 and, therefore, only a brief summary is presented herein.

The heat-transfer relations are found in terms of the Nusselt number $N_{Nu,i}$, Reynolds number R_i, and Prandtl number $N_{Pr,i}$ which are defined at the interface as follows:

$$N_{Nu,i}=\frac{x}{T_e-T_i}\left(\frac{dT}{dy}\right)_i$$

$$R_i=\frac{C\rho_i}{\mu_i}x^2$$

$$N_{Pr,i}=\frac{\mu_i}{k_i}c_{p,2}$$

In addition, the Schmidt number is defined as

$$N_{Sc,i}=\frac{\mu_i}{\rho_i D_{12}}$$

The rate of heat transfer to the interface q_i is then given by

$$q_i=\left(k\frac{dT}{dy}\right)_i=c_{p,2}(T_e-T_i)(\rho_i\mu_i C)^{1/2}\frac{1}{N_{Pr,i}}\frac{N_{Nu,i}}{R_i^{1/2}} \tag{21}$$

The following results (eqs. (22) to (29)) are taken directly from the analyses of references 4 and 5 (where the subscript 0 denotes no vaporization):

For axisymmetric flow with constant $\rho\mu$,

$$\frac{1}{N_{Pr,i}}\left(\frac{N_{Nu,i}}{R_i^{1/2}}\right)_0=\left[0.765-0.065\left(1-\frac{T_i}{T_e}\right)\right]N_{Pr,i}^{-0.6} \tag{22a}$$

and for two-dimensional flow with constant $\rho\mu$,

$$\frac{1}{N_{Pr,i}}\left(\frac{N_{Nu,i}}{R_i^{1/2}}\right)_0=\left[0.570-0.065\left(1-\frac{T_i}{T_e}\right)\right]N_{Pr,i}^{-0.6} \tag{22b}$$

For axisymmetric flow with variable $\rho\mu$,

$$\frac{1}{N_{Pr,i}}\left(\frac{N_{Nu,i}}{R_i^{1/2}}\right)_0=0.765\left(\frac{\rho_e\mu_e}{\rho_i\mu_i}\right)^{0.4}N_{Pr,i}^{-0.6} \tag{23a}$$

and for two-dimensional flow with variable $\rho\mu$,

$$\frac{1}{N_{Pr,i}}\left(\frac{N_{Nu,i}}{R_i^{1/2}}\right)_0=0.570\left(\frac{\rho_e\mu_e}{\rho_i\mu_i}\right)^{0.4}N_{Pr,i}^{-0.6} \tag{23b}$$

Equation (23a) is essentially that used in reference 6 for an equilibrium gas with a Lewis number of unity. Results given by equation (23a) are compared with the exact results of reference 7 in figure 2. The effect of mass transfer by vaporization across the interface is given by

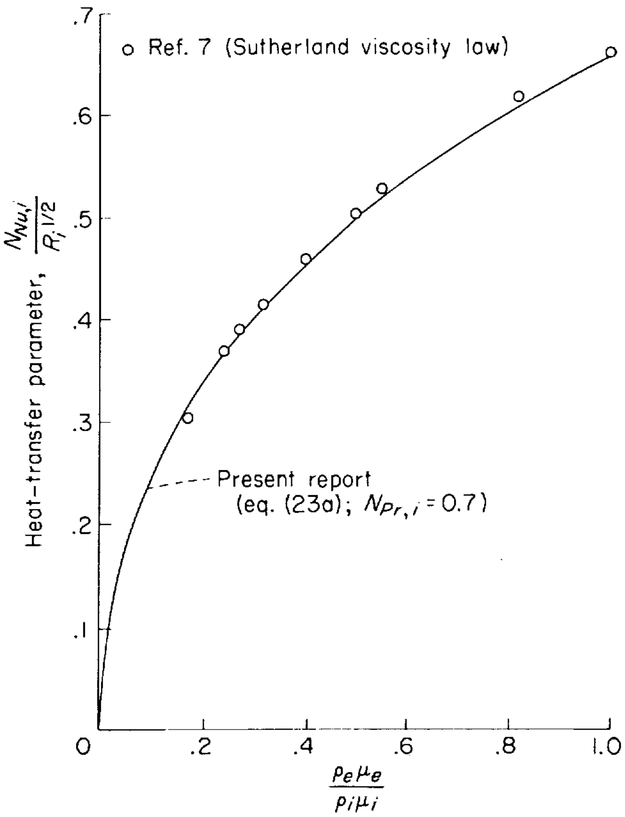

FIGURE 2.—Variation of $\frac{N_{Nu,i}}{R_i^{1/2}}$ with $\frac{\rho_e\mu_e}{\rho_i\mu_i}$. Axisymmetric stagnation point; no vaporization.

$$\frac{1}{N_{Pr,i}}\frac{N_{Nu,i}}{R_i^{1/2}}=\left(\frac{1}{N_{Pr,i}}\frac{N_{Nu,i}}{R_i^{1/2}}\right)_0-\left(1-\frac{1}{3}N_{Pr,i}^{-0.6}\right)\left[1+\left(\frac{c_{p,1}}{c_{p,2}}-1\right)\overline{W}\right]\frac{\dot{m}_i}{(\rho_i\mu_i C)^{1/2}} \tag{24}$$

where $\overline{W}$ is the mean concentration of foreign gas in the boundary layer and is given in reference 4 as a function of $N_{Sc,i}$. Equation (24) is valid for both two-dimensional and axisymmetric flows. The last term in equation (24) represents the reduction in the rate of heat transfer due to the shielding effect of the mixture of air and gas in the boundary layer. A comparison of the results given by equation (24) with the exact results of reference 7 for the special case $c_{p,1}=c_{p,2}$ is shown in figure 3 for both variable and constant $\rho\mu$.

The thickness of the velocity boundary layer with no vaporization $\delta_{u,0}$ is given in dimensionless form as

$$\delta_{u,0}\left(\frac{\rho_i C}{\mu_i}\right)^{1/2}=6\left(\frac{N_{Nu,i}}{R_i^{1/2}}\right)_0^{(1)} \tag{25}$$

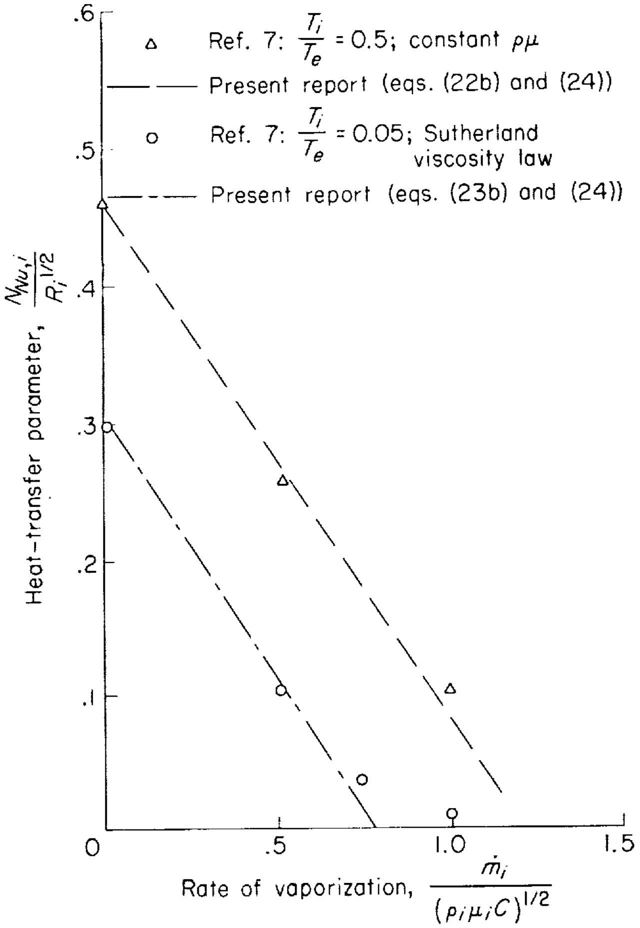

FIGURE 3.—Effect of vaporization on heat-transfer parameter for two-dimensional flow. $c_{p,1}=c_{p,2}$; $N_{Pr,i}=0.7$.

where the superscript (1) denotes $N_{Pr,i}=1$. The increase in boundary-layer thickness due to mass transfer across the interface is given by

$$\delta_u=\delta_{u,0}+\frac{2\dot{m}_i}{\rho_i C} \tag{26}$$

The thermal-boundary-layer thickness δ_T and the concentration-boundary-layer thickness δ_W are given in terms of the velocity-boundary-layer thickness δ_u as follows:

$$\left.\begin{aligned} \frac{\delta_T}{\delta_u}&=N_{Pr,i}{}^{-0.3}\\ \frac{\delta_W}{\delta_u}&=N_{Sc,i}{}^{-0.3} \end{aligned}\right\} \tag{27}$$

The concentration of foreign gas at the interface W_i is given by

$$W_i=\frac{N_{Sc,i}{}^{0.6}\dfrac{\dot{m}_i}{(\rho_i\mu_i C)^{1/2}}}{\left(\dfrac{N_{Nu,i}}{R_i^{1/2}}\right)_0^{(1)}+\dfrac{1}{3}\dfrac{\dot{m}_i}{(\rho_i\mu_i C)^{1/2}}} \tag{28}$$

From equation (28) it is seen that W_i increases with $\frac{\dot{m}_i}{(\rho_i\mu_i C)^{1/2}}$ and reaches the value of unity when

$$\frac{\dot{m}_i}{(\rho_i\mu_i C)^{1/2}}=\frac{\left(\dfrac{N_{Nu,i}}{R_i^{1/2}}\right)_0^{(1)}}{N_{Sc,i}{}^{0.6}-\dfrac{1}{3}}$$

When $W_i=1$, however, equation (16) shows that $T_i=T_B$, that is, the liquid at the interface has reached the boiling temperature. Since W_i cannot increase above unity (by definition), equation (28) ceases to be true for

$$\frac{\dot{m}_i}{(\rho_i\mu_i C)^{1/2}}>\frac{\left(\dfrac{N_{Nu,i}}{R_i^{1/2}}\right)_0^{(1)}}{N_{Sc,i}{}^{0.6}-\dfrac{1}{3}}=\frac{\dot{m}_{i,B}}{(\rho_i\mu_i C)^{1/2}}$$

The boundary condition given by equation (15) also shows that $\frac{\dot{m}_i}{(\rho_i\mu_i C)^{1/2}}$ and W_i are not related when $W_i=1$ since equation (15) is satisfied for arbitrary values of $\dot{m}_i$. This is to be expected physically when the boiling temperature is reached.

The heat-transfer relation given by equation (24) is modified when $\dot{m}_i>\dot{m}_{i,B}$ and is now obtained by the method of reference 5 as follows: The integral equation (13) of reference 5 is first written in the dimensionless form

$$\begin{aligned}\delta_u\left(\frac{\rho_i C}{\mu_i}\right)^{1/2}&\left[\frac{1}{\delta_u}\int_0^z\frac{T_e-T}{T_e-T_i}\frac{u}{U}\,dz\right.\\&\left.+\left(\frac{c_{p,1}}{c_{p,2}}-1\right)\frac{W_i}{\delta_u}\int_0^z\frac{W}{W_i}\frac{T_e-T}{T_e-T_i}\frac{u}{U}\,dz\right]\\&=\frac{1}{N_{Pr,i}}\frac{N_{Nu,i}}{R_i^{1/2}}+\left(\frac{c_{p,1}}{c_{p,2}}-1\right)\frac{\dot{m}_i}{(\rho_i\mu_i C)^{1/2}}+\frac{\dot{m}_i}{(\rho_i\mu_i C)^{1/2}}\end{aligned}$$

Substitution into this equation of $W_i=1$ and

$$\frac{1}{6}\delta_u\left(\frac{\rho_i C}{\mu_i}\right)^{1/2}=N_{Pr,i}{}^{0.6}\left(\frac{1}{N_{Pr,i}}\frac{N_{Nu,i}}{R_i^{1/2}}\right)_0+\frac{1}{3}\frac{\dot{m}_i}{(\rho_i\mu_i C)^{1/2}}$$

(from eqs. (23), (24), and (26) of ref. 5) and the linear profiles given by equations (21) and (38) of reference 5 yields

$$\frac{1}{N_{Pr,i}}\frac{N_{Nu,i}}{R_i^{1/2}}=\left(\frac{1}{N_{Pr,i}}\frac{N_{Nu}}{R_i^{1}}\right)_0$$
$$-\left(1-\frac{1}{3}N_{Pr,i}^{-0.6}\right)\frac{\dot{m}_i}{(\rho_i\mu_iC)^{1/2}}$$
$$-\left(\frac{c_{p,1}}{c_{p,2}}-1\right)(1-KN_{Sc,i}^{0.6})-\left(\frac{c_{p,1}}{c_{p,2}}-1\right)$$
$$KN_{Sc,i}^{0.6}\left[1-\frac{N_{Sc,i}^{-0.6}}{6}\delta_u\left(\frac{\rho_iC}{\mu_i}\right)^{1/2}\frac{(\rho_i\mu_iC)^{1/2}}{\dot{m}_i}\right]$$

where K is defined by equation (40) of reference 5. Finally, substitution for K from equation (42) of reference 5 gives the form

$$\frac{1}{N_{Pr,i}}\frac{N_{Nu,i}}{R_i^{1/2}}=\left(\frac{1}{N_{Pr,i}}\frac{N_{Nu,i}}{R_i^{1/2}}\right)_0$$
$$-\left(1-\frac{1}{3}N_{Pr,i}^{-0.6}\right)\left[1+\left(\frac{c_{p,1}}{c_{p,2}}-1\right)\overline{W}\right]\frac{\dot{m}_i}{(\rho_i\mu_iC)^{1/2}}$$
$$-J\left(1-\frac{1}{3}N_{Pr,i}^{-0.6}\right)\frac{\dot{m}_i}{(\rho_i\mu_iC)^{1/2}}\qquad\text{(29a)}$$

where

$$J=\left(\frac{c_{p,1}}{c_{p,2}}-1\right)\left[\left(N_{Sc,i}^{0.6}-\frac{1}{3}\right)\right.$$
$$\left.-\frac{(\rho_i\mu_iC)^{1/2}}{\dot{m}_i}\left(\frac{N_{Nu,i}}{R_i^{1/2}}\right)_0^{(1)}\right]N_{Sc,i}^{-0.6}\left[1\right.$$
$$\left.-\left(1-\frac{1}{3}N_{Pr,i}^{-0.6}\right)\overline{W}\right]\qquad\text{(29b)}$$

and represents the additional effect due to the boiling; the term is positive for $c_{p,1}>c_{p,2}$ and negative for $c_{p,1}<c_{p,2}$.

Skin friction.—The value of the skin friction which results when there is no mass transfer across the interface is first obtained by utilizing available exact solutions.

The integral form of the momentum equation near the stagnation point is for axisymmetric flow

$$\frac{\rho_i}{\rho_e}\left[\frac{1}{U}\frac{dU}{dx}(3\Delta_m+\Delta^*)\right]=\frac{\mu_i}{\rho_eU^2}\left(\frac{\partial u}{\partial y}\right)_i+\frac{\rho_i}{\rho_e}\frac{v_i}{U}$$

and for two-dimensional flow

$$\frac{\rho_i}{\rho_e}\left[\frac{1}{U}\frac{dU}{dx}(2\Delta_m+\Delta^*)\right]=\frac{\mu_i}{\rho_eU^2}\left(\frac{\partial u}{\partial y}\right)_i+\frac{\rho_i}{\rho_e}\frac{v_i}{U}$$

which may be written

$$I=\frac{1}{\delta_u}\left(\frac{\mu_i}{\rho_iC}\right)^{1/2}\left[\frac{\mu_i}{(\rho_i\mu_iC)^{1/2}}\frac{\partial}{\partial y}\left(\frac{u}{U}\right)_i+\frac{\dot{m}_i}{(\rho_i\mu_iC)^{1/2}}\right]\qquad\text{(30)}$$

where for axisymmetric flow

$$I=3\frac{\Delta_m}{\delta_u}+\frac{\Delta^*}{\delta_u}\qquad\text{(31a)}$$

and for two-dimensional flow

$$I=2\frac{\Delta_m}{\delta_u}+\frac{\Delta^*}{\delta_u}\qquad\text{(31b)}$$

In equations (31),

$$\Delta_m=\int_0^Z\frac{u}{U}\left(1-\frac{u}{U}\right)dz$$

$$\Delta^*=\int_0^Z\left(1-\frac{u}{U}\right)dz-\int_0^Z\left(1-\frac{\rho_e}{\rho}\right)dz$$

and

$$\delta_u=\int_0^\delta\frac{\rho}{\rho_i}dy'$$

where $z=\int_0^{y'}\frac{\rho}{\rho_i}dy'$ and Z is some arbitrary value of z outside the boundary layer. The quantity Δ_m is the momentum thickness and Δ^* is the displacement thickness, based on a reference density ρ_i. The dimensionless ratios Δ_m/δ_u and Δ^*/δ_u, and hence I, are independent of the reference density, however.

It is seen that I is a dimensionless quantity which depends on the details of the boundary-layer profiles; the method used herein to determine the effect of mass transfer on the skin friction (similar to that used in refs. 4 and 5 to determine the effect of mass transfer on heat transfer) avoids the evaluation of I. Firstly, it is convenient to express equation (30) in terms of the Reynolds number and skin-friction coefficient

$$C_f=\frac{\tau_i}{\frac{1}{2}\rho_iU^2}=\frac{\mu_i\left(\frac{\partial u}{\partial y}\right)_i}{\frac{1}{2}\rho_iU^2}\qquad\text{(32a)}$$

Equation (32a) can be expressed by use of the definition of R_i in the alternative form

$$\frac{1}{2}C_fR_i^{1/2}=\frac{\tau_i}{(\rho_i\mu_iC)^{1/2}}\frac{1}{Cx}\qquad\text{(32b)}$$

With these dimensionless coefficients equation (30) becomes

$$I=\frac{1}{\delta_u\left(\frac{\rho_iC}{\mu_i}\right)^{1/2}}\left[\frac{1}{2}C_fR_i^{1/2}+\frac{\dot{m}_i}{(\rho_i\mu_iC)^{1/2}}\right]\qquad\text{(33)}$$

The dimensionless thickness $\delta_u\left(\frac{\rho_i C}{\mu_i}\right)^{1/2}$ is already known and is given by equations (25) and (26).

The skin-friction parameter $\left(\frac{1}{2}C_f R_i^{1/2}\right)_0$ is known from exact calculations (ref. 7) and was found to satisfy approximately the following equations:
For axisymmetric flow with constant $\rho\mu$,

$$\left(\frac{1}{2}C_f R_i^{1/2}\right)_0=1.312-0.489\left(1-\frac{T_i}{T_e}\right) \tag{34}$$

and for two-dimensional flow with constant $\rho\mu$,

$$\left(\frac{1}{2}C_f R_i^{1/2}\right)_0=1.233-0.626\left(1-\frac{T_i}{T_e}\right) \tag{35}$$

where the subscript 0 implies no mass transfer. The small variations with Prandtl number in this parameter have been neglected.

A simple power law for the variation of the skin-friction parameter with $\rho\mu$ was sought, similar to that for the heat-transfer coefficient (eqs. (23a) and (23b)) and valid in the range

$$T_e=10{,}000^\circ\text{ R}\qquad\left(0.5<\frac{T_i}{T_e}<0.05\right)$$

and

$$T_e=2{,}000^\circ\text{ R}\qquad\left(0.5<\frac{T_i}{T_e}<0.2\right)$$

(The Sutherland viscosity law $\mu\propto\frac{T^{3/2}}{T+Su}$ with $Su=200^\circ$ R was used.)

The following results were obtained from the exact solutions of reference 7 (and from interpolation of these solutions):
For axisymmetric flow with variable $\rho\mu$,

$$\left(\frac{1}{2}C_f R_i^{1/2}\right)_0=1.21\left(\frac{\rho_e\mu_e}{\rho_i\mu_i}\right)^{0.6} \tag{36}$$

and for two-dimensional flow with variable $\rho\mu$,

$$\left(\frac{1}{2}C_f R_i^{1/2}\right)_0=1.02\left(\frac{\rho_e\mu_e}{\rho_i\mu_i}\right)^{0.6} \tag{37}$$

In figure 4 is presented a comparison between the results obtained by use of equations (36) and (37) and those of reference 7.

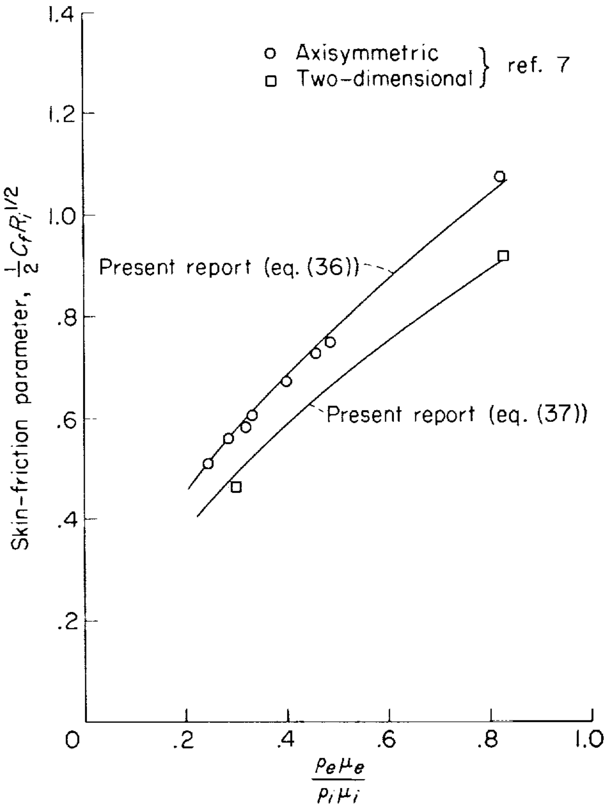

FIGURE 4.—Variation of skin-friction parameter with $\frac{\rho_e\mu_e}{\rho_i\mu_i}$. No vaporization.

The reduction of skin friction at the interface as a result of mass transfer across the interface is now found. It is assumed that, when mass transfer takes place, the momentum thickness and the displacement thickness are increased in proportion to the increase in δ_u; thus, $\frac{\Delta_m}{\delta_u}$ and $\frac{\Delta^*}{\delta_u}$, and hence I, are assumed to remain unchanged.

Equations (26) and (33) then give

$$\frac{1}{\delta_{u,0}}\left(\frac{\mu_i}{\rho_i C}\right)^{1/2}\left(\frac{1}{2}C_f R_i^{1/2}\right)_0=\frac{\frac{1}{2}C_f R_i^{1/2}+\frac{\dot{m}_i}{(\rho_i\mu_i C)^{1/2}}}{\delta_{u,0}\left(\frac{\rho_i C}{\mu_i}\right)^{1/2}+\frac{2\dot{m}_i}{(\rho_i\mu_i C)^{1/2}}} \tag{38}$$

When expression (25) with the relevant equation of equations (22a) to (23b) is used for $\delta_{u,0}\left(\frac{\mu_i}{\rho_i C}\right)^{1/2}$ and the relevant equation of equations (34) to

(37) is used for $\left(\frac{1}{2}C_fR_i^{1/2}\right)_0$, then equation (38) gives the following expressions for the skin-friction parameter $\frac{1}{2}C_fR_i^{1/2}$ with mass transfer across the interface:

For axisymmetric flow with constant $\rho\mu$,

$$\frac{1}{2}C_fR_i^{1/2}=1.312-0.489\left(1-\frac{T_i}{T_e}\right)-\frac{\dot{m}_i}{(\rho_i\mu_iC)^{1/2}}\left[1-\frac{1}{3}\,\frac{1.312-0.489\left(1-\frac{T_i}{T_e}\right)}{0.765-0.065\left(1-\frac{T_i}{T_e}\right)}\right] \qquad (39)$$

and for two-dimensional flow with constant $\rho\mu$,

$$\frac{1}{2}C_fR_i^{1/2}=1.233-0.626\left(1-\frac{T_i}{T_e}\right)-\frac{\dot{m}_i}{(\rho_i\mu_iC)^{1/2}}\left[1-\frac{1}{3}\,\frac{1.233-0.626\left(1-\frac{T_i}{T_e}\right)}{0.570-0.065\left(1-\frac{T_i}{T_e}\right)}\right] \qquad (40)$$

The results given by equation (40) are compared with the exact results of reference 7 in figure 5.

The relations derived for constant $\rho\mu$ (eqs. (39) and (40)) are presented only for the purpose

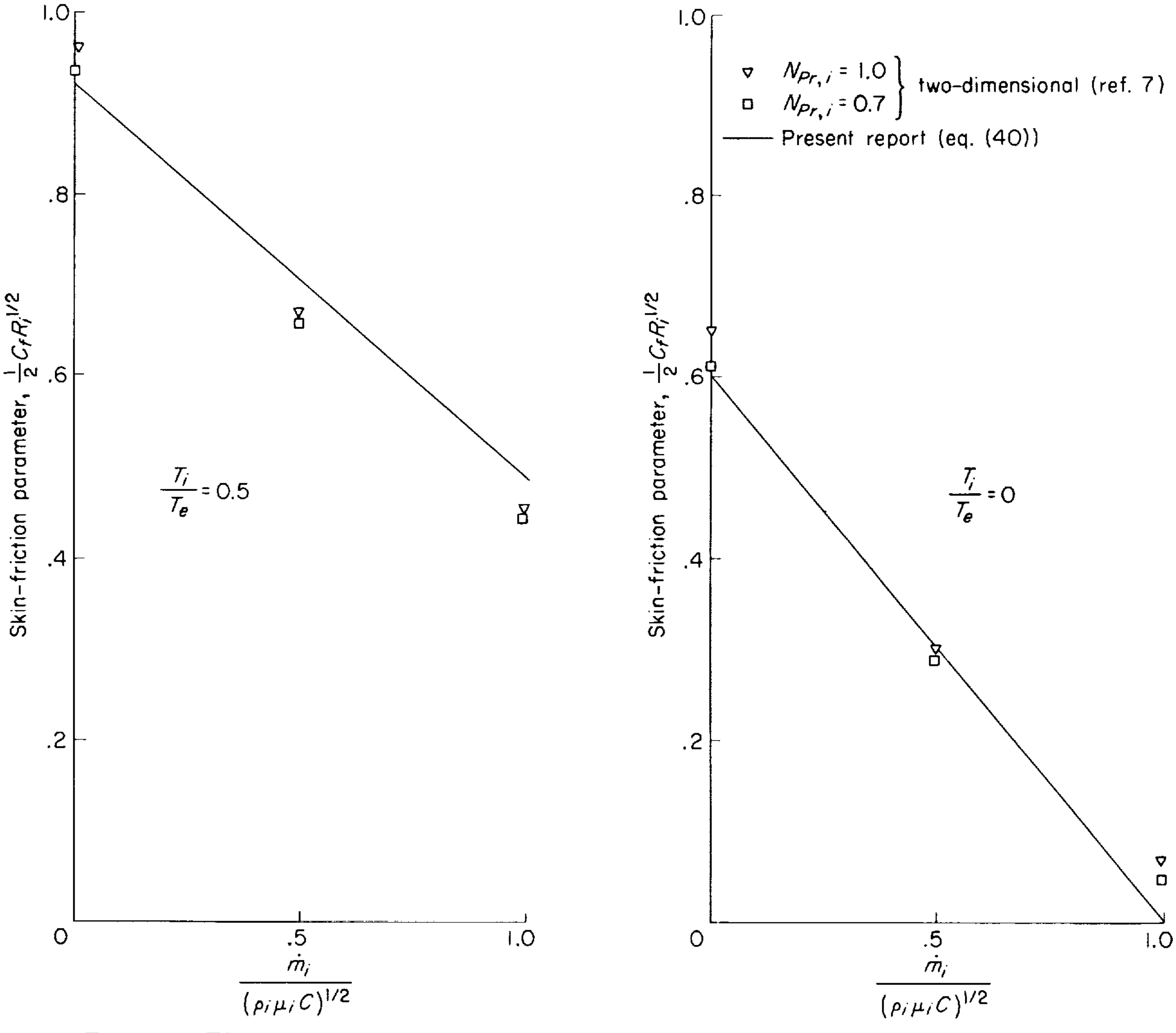

FIGURE 5.—Effect of vaporization on skin-friction parameter for two-dimensional flow. $\rho\mu$ constant.

of comparison with exact solutions as an additional check on the validity of the simplified approach used in this report. In the rest of the report only those expressions in which $\rho\mu$ is variable are used.

For axisymmetric flow with variable $\rho\mu$,

$$\frac{1}{2}C_fR_i^{1/2}=1.21\left(\frac{\rho_e\mu_e}{\rho_i\mu_i}\right)^{0.6}-\frac{\dot{m}_i}{(\rho_i\mu_iC)^{1/2}}\left[1-\frac{1}{3}\frac{1.21}{0.765}\left(\frac{\rho_e\mu_e}{\rho_i\mu_i}\right)^{0.2}\right] \tag{41}$$

and for two-dimensional flow with variable $\rho\mu$,

$$\frac{1}{2}C_fR_i^{1/2}=1.02\left(\frac{\rho_e\mu_e}{\rho_i\mu_i}\right)^{0.6}-\frac{\dot{m}_i}{(\rho_i\mu_iC)^{1/2}}\left[1-\frac{1}{3}\frac{1.02}{0.570}\left(\frac{\rho_e\mu_e}{\rho_i\mu_i}\right)^{0.2}\right] \tag{42}$$

A comparison of the results given by equation (42) with the exact results of reference 7 is shown in figure 6. Again it is seen that the present method gives numerical results accurate enough for engineering calculations.

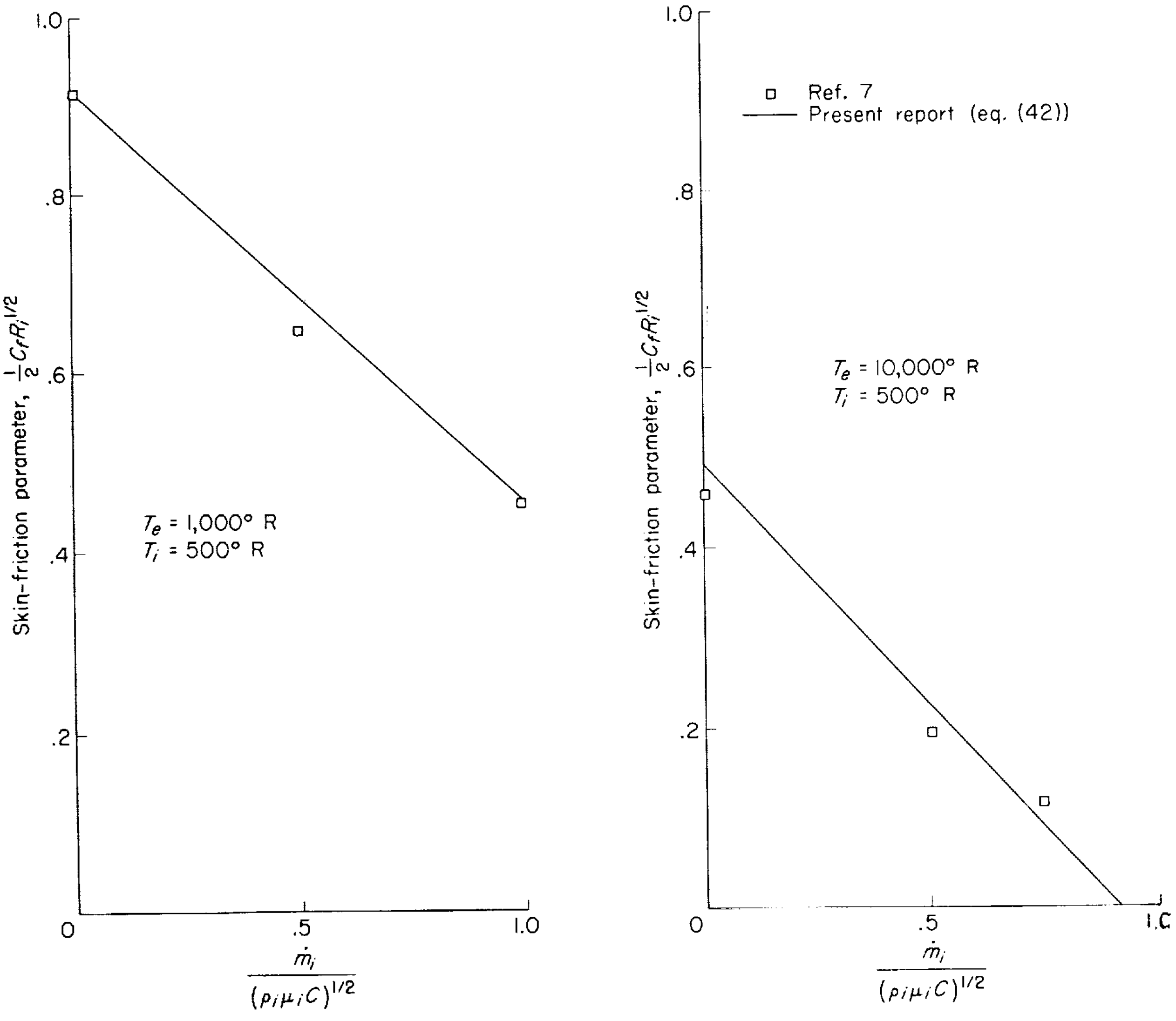

FIGURE 6.—Effect of vaporization on skin-friction parameter for two-dimensional flow. $N_{Pr,i}=0.7$. $\rho\mu$ variable.

Now that the heat-transfer rate and skin friction are known in terms of $\dot m_i$ attention is turned to the liquid layer.

FLOW IN THE LIQUID LAYER

The mass balance in the liquid layer is written for the axisymmetric case as

$$\dot m = 2C_l\int_0^D \rho_l \frac{u}{u_{l,i}}\,dy+\dot m_i \tag{43}$$

and for the two-dimensional case as

$$\underbrace{\dot m}_{\text{Mass lost by solid}} = \underbrace{C_l\int_0^D \rho_l \frac{u}{u_{l,i}}\,dy}_{\text{Mass convected in liquid layer}} + \underbrace{\dot m_i}_{\text{Mass transfer across interface}} \tag{44}$$

In equations (43) and (44), D is the thickness of the liquid layer.

The integral is evaluated by assuming a linear velocity profile

$$\frac{u}{u_{l,i}}=\frac{y}{D} \tag{45}$$

so that equation (43) for axisymmetric flow reduces to

$$\dot m-\dot m_i=C_l\rho_l D \tag{46}$$

and equation (44) for two-dimensional flow reduces to

$$\dot m-\dot m_i=\frac{1}{2}\,C_l\rho_l D \tag{47}$$

The heat-balance equation in the liquid layer is treated in a similar way:

For the axisymmetric case,

$$q_i=L_v\dot m_i+c_l(T_i-T_w)\dot m_i +2C_l\int_0^D c_l\rho_l(T-T_w)\frac{u}{u_{l,i}}\,dy+q_w \tag{48a}$$

and for the two-dimensional case,

$$\underbrace{q_i}_{\text{Heat transfer from gas layer}} = \underbrace{L_v\dot m_i}_{\text{Latent heat of vaporization}} + \underbrace{c_l(T_i-T_w)\dot m_i}_{\text{Heating before vaporization}} + \underbrace{C_l\int_0^D c_l\rho_l(T-T_w)\frac{u}{u_{l,i}}\,dy}_{\text{Convection of heat parallel to wall}} + \underbrace{q_w}_{\text{Heat transfer to wall}} \tag{48b}$$

where

$$q_w=\dot m[L_m+c_b(T_w-T_b)] \tag{49}$$

The integral in equations (48) is evaluated by use of the assumed linear temperature profile

$$\frac{T-T_w}{T_i-T_w}=\frac{y}{D} \tag{50}$$

Insertion of equation (45), either equation (46) or (47), and equation (50) into equation (48a) or equation (48b) gives the following result:

$$q_i=L_v\dot m_i+c_l(T_i-T_w)\dot m_i +\frac{2}{3}c_l(T_i-T_w)(\dot m-\dot m_i)+[L_m+c_b(T_w-T_b)]\dot m \tag{51}$$

that is, the mass $\dot m-\dot m_i$ removed as a liquid is raised through an effective temperature difference of $\frac{2}{3}\,(T_i-T_w)$ during convection. Equation (51) is valid for both two-dimensional and axisymmetric flows.

The rate at which mass is convected away from the vicinity of the stagnation point in liquid form depends on the velocity at the interface $u_{l,i}=C_l x$ and the thickness of the liquid layer D as shown by equation (46) or equation (47). These quantities depend on the shear stress at the interface which is approximated by

$$\tau_i=\left(\mu\frac{\partial u}{\partial y}\right)_{l,i}\approx\mu_{l,i}\frac{u_{l,i}}{D}=\mu_{l,i}\frac{C_l x}{D} \tag{52}$$

A comparison between the results obtained by use of the linear relation (52) and those obtained by using higher order profiles was made in reference 1 and showed virtually no change in the shielding effect of the liquid layer.

The relation between heat transfer across the liquid layer and the temperature difference is written in the approximate form as

$$k_l\,\frac{(T_i-T_w)}{D}=\frac{1}{2}\,(q_{l,i}+q_w) \tag{53}$$

which results from the assumption of a parabolic temperature profile. In equation (53)

$$\left.\begin{aligned} q_{l,i}&=c_l(T_i-T_w)\dot{m}_i+\frac{2}{3}c_l(T_i\\ &\qquad -T_w)(\dot{m}-\dot{m}_i)+q_w\\ q_w&=[L_m+c_b(T_w-T_b)]\dot{m}\end{aligned}\right\} \tag{54}$$

that is, $q_{l,i}$ and q_w are, respectively, the rates of heat transfer to the liquid layer at the interface and from the liquid layer at the wall.

APPLICATION OF THE INTERFACE BOUNDARY CONDITIONS

In the preceding sections expressions have been obtained for the shear stress and rate of heat transfer evaluated at both sides of the interface. The boundary conditions which relate corresponding quantities on either side of the interface are now applied.

From equations (14), (21), and (54),

$$\begin{aligned} c_{p,2}(T_e-T_i)(\rho_i\mu_iC)^{1/2}\left(\frac{1}{N_{Pr,i}}\frac{N_{Nu,i}}{R_i^{1/2}}\right)&\\ =[L_v+c_l(T_i-T_w)]\dot{m}_i+\frac{2}{3}c_l(T_i-T_w)(\dot{m}-\dot{m}_i)&\\ +[L_m+c_b(T_w-T_b)]\dot{m}& \end{aligned}\tag{55}$$

and from equations (18), (32), and (52),

$$\frac{1}{2}C_fR_i^{1/2}(\rho_i\mu_iC)^{1/2}Cx=\mu_{l,i}\frac{C_lx}{D} \tag{56}$$

The concentration W_i is eliminated from equations (16) and (28) to give

$$\frac{\left(\dfrac{N_{Nu,i}}{R_i^{1/2}}\right)_0^{(1)}+\dfrac{1}{3}\dfrac{\dot{m}_i}{(\rho_i\mu_iC)^{1/2}}}{N_{Sc,i}{}^{0.6}\dfrac{\dot{m}_i}{(\rho_i\mu_iC)^{1/2}}}=1+\frac{M_2}{M_1}\left(e^{\frac{L_v}{R_1}\left(\frac{1}{T_i}-\frac{1}{T_B}\right)}-1\right) \tag{57}$$

when $T_i<T_B$.

Equations (53) and (54) are combined in the form

$$\begin{aligned}\frac{k_l(T_i-T_w)}{D}=\frac{1}{2}c_l(T_i-T_w)\left(\frac{2}{3}\dot{m}+\frac{1}{3}\dot{m}_i\right)&\\ +[L_m+c_b(T_w-T_b)]\dot{m}&\end{aligned} \tag{58}$$

Thus, equation (46) (or eq. (47)) and equations (55) to (58) are five equations from which $\dot{m}$, $\dot{m}_i$, T_i, D, and $u_{l,i}=C_lx$ can be determined since the dimensionless parameters $\frac{1}{N_{Pr,i}}\frac{N_{Nu,i}}{R_i^{1/2}}$ and $\frac{1}{2}C_fR_i^{1/2}$ are already known in terms of $\frac{\dot{m}_i}{(\rho_i\mu_iC)^{1/2}}$ through equations (23a) (or eq. (23b)), (24), and (41) (or eq. (42)).

The rates of mass loss $\dot{m}$ and $\dot{m}_i$ have been made dimensionless by the factor $(\rho_i\mu_iC)^{1/2}$ in order to compare the present method with previous exact results. It is more convenient, however, to use the quantity $(\rho_e\mu_eC)^{1/2}$ for this purpose; as will be seen later, the use of $(\rho_e\mu_eC)^{1/2}$ leads to some simplification of the analysis and presentation. Accordingly, equations (46) (or eq. (47)) and (55) to (58) are rewritten in terms of $\frac{\dot{m}}{(\rho_e\mu_eC)^{1/2}}$, $\frac{\dot{m}_i}{(\rho_e\mu_eC)^{1/2}}$, T_i, and $D\left(\frac{\rho_eC}{\mu_{l,i}}\right)^{1/2}$. Thus, from equations (55), (29), and (23a) (or eq. (23b)),

$$Q_0=Q_1\frac{(\dot{m}-\dot{m}_i)}{(\rho_e\mu_eC)^{1/2}}+(Q_2+Q_3)\frac{\dot{m}_i}{(\rho_e\mu_eC)^{1/2}} \tag{59}$$

where

$$Q_0=\alpha_1N_{Pr,i}{}^{-0.6}c_{p,2}(T_c-T_i) \tag{60a}$$

and, for the axisymmetric case,

$$\alpha_1=0.765\left(\frac{\rho_e\mu_e}{\rho_i\mu_i}\right)^{-0.1} \tag{60b}$$

and, for the two-dimensional case,

$$\alpha_1=0.570\left(\frac{\rho_e\mu_e}{\rho_i\mu_i}\right)^{-0.1} \tag{60c}$$

and

$$Q_1=c_b(T_w-T_b)+L_m+\frac{2}{3}c_l(T_i-T_w) \tag{60d}$$

$$Q_2=c_b(T_w-T_b)+L_m+c_l(T_i-T_w) \tag{60e}$$

$$Q_3=L_v+(\bar{c}_p+Jc_{p,2})\left(1-\frac{1}{3}N_{Pr,i}{}^{-0.6}\right)(T_e-T_i) \tag{60f}$$

where

$$\bar{c}_p=c_{p,1}\overline{W}+c_{p,2}(1-\overline{W}) \tag{61}$$

and, for $T_i<T_B$,

$$J=0$$

It is seen that Q_0 is associated with the rate of heat transfer to a nonablating body at a surface temperature T_i; Q_1 is the total heat absorbed when unit mass of liquid is removed, $\frac{2}{3}(T_i-T_w)$ being the mean temperature rise, Q_2 is that absorbed by unit mass before vaporization, and Q_3 is that absorbed during and after vaporization.

Elimination of C_l from equation (46) (or eq. (47)) and equation (56) with the aid of equation (41) (or eq. (42)) gives

$$\alpha_2 \frac{1-\alpha_3 \dfrac{\dot{m}_i}{(\rho_e\mu_e C)^{1/2}}}{\dfrac{\dot{m}-\dot{m}_i}{(\rho_e\mu_e C)^{1/2}}}=\left[D\left(\frac{\rho_l C}{\mu_{l,i}}\right)^{1/2}\right]^{-2} \tag{62}$$

where, for the axisymmetric case,

$$\alpha_2=1.21\left(\frac{\rho_e\mu_e}{\rho_i\mu_i}\right)^{0.1} \tag{63a}$$

for the two-dimensional case,

$$\alpha_2=0.51\left(\frac{\rho_e\mu_e}{\rho_i\mu_i}\right)^{0.1} \tag{63b}$$

for the axisymmetric case,

$$\alpha_3=\frac{1-\dfrac{1}{3}\dfrac{1.21}{0.765}\left(\dfrac{\rho_e\mu_e}{\rho_i\mu_i}\right)^{0.2}}{1.21\left(\dfrac{\rho_e\mu_e}{\rho_i\mu_i}\right)^{0.1}} \tag{64a}$$

and, for the two-dimensional case,

$$\alpha_3=\frac{1-\dfrac{1}{3}\dfrac{1.02}{0.570}\left(\dfrac{\rho_e\mu_e}{\rho_i\mu_i}\right)^{0.2}}{1.02\left(\dfrac{\rho_e\mu_e}{\rho_i\mu_i}\right)^{0.1}} \tag{64b}$$

Equation (58) is written by use of the definition $N_{Pr,l,i}=\frac{\mu_{l,i}C_l}{k_l}$ as

$$\frac{1}{N_{Pr,l,i}}\left[D\left(\frac{\rho_l C}{\mu_{l,i}}\right)^{1/2}\right]^{-1}\left(\frac{\rho_l\mu_{l,i}}{\rho_e\mu_e}\right)^{1/2}=\frac{1}{6}\frac{\dot{m}_i}{(\rho_e\mu_e C)^{1/2}} +\left[\frac{1}{3}+\frac{L_m+c_b(T_w-T_b)}{c_l(T_i-T_w)}\right]\frac{\dot{m}}{(\rho_e\mu_e C)^{1/2}} \tag{65}$$

and equation (57) becomes

$$\frac{\alpha_1+\dfrac{1}{3}\dfrac{\dot{m}_i}{(\rho_e\mu_e C)^{1/2}}}{N_{Sc,i}{}^{0.6}\dfrac{\dot{m}_i}{(\rho_e\mu_e C)^{1/2}}}=1+\frac{M_2}{M_1}\left(e^{\frac{L_v}{R_1}\left(\frac{1}{T_i}-\frac{1}{T_B}\right)}-1\right) \tag{66}$$

where α_1 is defined by either equation (60b) or equation (60c).

From equations (59), (62), (65), and (66) the four quantities $\frac{\dot{m}}{(\rho_e\mu_e C)^{1/2}}$, $\frac{\dot{m}_i}{(\rho_e\mu_e C)^{1/2}}$, T_i, and $D\left(\frac{\rho_l C}{\mu_{l,i}}\right)^{1/2}$ can be determined.

The detailed results obtained from these equations depend on the numerical values of the thermal and diffusive parameters involved; however, some general results are easily obtained upon examination of the equations.

RESULTS AND DISCUSSION

INTERFACE TEMPERATURE T_i

It is noteworthy that for small values of $\frac{\dot{m}_i}{(\rho_e\mu_e C)^{1/2}}$, that is, for the lower range of T_e, there is a single relation between the external temperature T_e and the interface temperature T_i which holds for both axisymmetric and two-dimensional flows. This is seen when $\frac{\dot{m}_i}{(\rho_e\mu_e C)^{1/2}}$ is made equal to zero in equations (59), (62), and (65) and the quantities $\frac{\dot{m}}{(\rho_e\mu_e C)^{1/2}}$ and $D\left(\frac{\rho_l C}{\mu_{l,i}}\right)^{1/2}$ are eliminated; the result is

$$\frac{c_{p,2}(T_e-T_i)}{c_b(T_w-T_b)+L_m+\frac{2}{3}c_l(T_i-T_w)}\left(\frac{\rho_e\mu_e}{\rho_l\mu_{l,i}}\right)^{1/3} =\alpha_4\frac{N_{Pr,i}{}^{0.6}}{N_{Pr,l,i}{}^{2/3}}\left[\frac{c_l(T_i-T_w)}{c_b(T_w-T_b)+L_m+\frac{1}{3}c_l(T_i-T_w)}\right]^{2/3} \tag{67}$$

where, for the axisymmetric case,

$$\alpha_4=\frac{(1.21)^{1/3}}{0.765}\left(\frac{\rho_e\mu_e}{\rho_i\mu_i}\right)^{0.133} \tag{68}$$

and, for the two-dimensional case,

$$\alpha_4=\frac{(0.51)^{1/3}}{0.570}\left(\frac{\rho_e\mu_e}{\rho_i\mu_i}\right)^{0.133} \tag{69}$$

The numerical factors in the expressions for α_4 are both 1.4 (with an error of less than 1/2 percent); thus equation (67) with $\alpha_4=1.4\left(\frac{\rho_e\mu_e}{\rho_i\mu_i}\right)^{0.133}$ is a single relation between T_e and T_i since the quantities $\frac{\rho_e\mu_e}{\rho_l\mu_{l,i}}$ and $\frac{\rho_e\mu_e}{\rho_i\mu_i}$ depend only on T_i and T_e.

Furthermore, in the range of high values of

$T_e - T_i$ where the condition

$$\frac{c_b(T_w - T_b) + L_m + c_l(T_i - T_w)}{c_{p,2}(T_e - T_i)} << 1$$

applies $\left(\text{but } \frac{\dot{m}_i}{(\rho_e \mu_e C)^{1/2}} \text{ is not negligible}\right)$, the terms Q_1 and Q_2 may be neglected and equation (59) has the approximate form, for $T_i < T_B$,

$$N_{Pr,i}^{-0.6} c_{p,2}(T_e - T_i) = \left[L_v + \bar{c}_p \left(1 - \frac{1}{3} N_{Pr,i}^{-0.6}\right)(T_e - T_i)\right] \frac{\dot{m}_i}{(\rho_e \mu_e C)^{1/2}} \quad (70)$$

Equation (66) is written

$$\frac{1 + \frac{1}{3} \frac{\dot{m}_i}{\alpha_1 (\rho_e \mu_e C)^{1/2}}}{N_{Sc,i}^{0.6} \frac{\dot{m}_i}{\alpha_1 (\rho_e \mu_e C)^{1/2}}} = 1 + \frac{M_2}{M_1}\left(e^{\frac{L_v}{R_1}\left(\frac{1}{T_i} - \frac{1}{T_B}\right)} - 1\right) \quad (71)$$

and elimination of the quantity $\frac{\dot{m}_i}{\alpha_1 (\rho_e \mu_e C)^{1/2}}$ gives a relation between T_e and T_i which is independent of α_1 and is therefore valid for both axisymmetric and two-dimensional flows; that is,

$$\frac{L_v}{c_{p,2}(T_e - T_i) N_{Pr,i}^{-0.6}} = \frac{M_2}{M_1}\left(e^{\frac{L_v}{R_1}\left(\frac{1}{T_i} - \frac{1}{T_B}\right)} - 1\right) N_{Sc,i}^{0.6} + \left(N_{Sc,i}^{0.6} - \frac{1}{3}\right) - \frac{\bar{c}_p}{c_{p,2}}\left(N_{Pr,i}^{0.6} - \frac{1}{3}\right) \quad (72)$$

(Even when the dependence of $N_{Sc,i}$ and $N_{Pr,i}$ on W_i is considered, it may be shown that W_i itself depends on $\frac{\dot{m}_i}{\alpha_1 (\rho_e \mu_e C)^{1/2}}$ through equation (28); thus, α_1 is eliminated with $\dot{m}_i$ and equation (72) still does not contain α_1.)

It is therefore expected that in general the interface temperature T_i (for a given material) depends only on the external temperature T_e and is the same for both axisymmetric and two-dimensional bodies.

LIQUID BOILING

Another result of importance is obtained when it is noted that equation (72) gives the conditions under which possible boiling of the liquid occurs. As $T_i \rightarrow T_B$, equation (72) reduces to

$$\frac{L_v}{c_{p,2}(T_e - T_i) N_{Pr,i}^{-0.6}} = \left(N_{Sc,i}^{0.6} - \frac{1}{3}\right) - \frac{\bar{c}_p}{c_{p,2}}\left(N_{Pr,i}^{0.6} - \frac{1}{3}\right) \quad (73)$$

From equation (73) it is seen that it is not always possible for boiling to occur, for if

$$\frac{\bar{c}_p}{c_{p,2}} > \frac{N_{Sc,i}^{0.6} - \frac{1}{3}}{N_{Pr,i}^{0.6} - \frac{1}{3}} \quad (74)$$

the right-hand side of equation (73) assumes negative values and the equation cannot be satisfied; thus, equation (74) gives the condition under which boiling cannot occur—that is, when

(a) $\bar{c}_p / c_{p,2}$ is sufficiently large or
(b) $N_{Pr,i}$ is sufficiently large or
(c) $N_{Sc,i}$ is sufficiently small.

These conditions are precisely those which give maximum shielding by the gas layer (ref. 4). It is noteworthy that the condition for boiling depends only on the thermal and diffusive properties of the ablation material in the gaseous state; it is independent of the nose curvature, the pressure, the heat-transfer parameter, and the boiling temperature of the liquid.

Figure 7 shows the range of $N_{Pr,i}$ and $N_{Sc,i}$ in which boiling is possible. For any given value of $\frac{c_{p,1}}{c_{p,2}}$ boiling is possible in the region above the line but is not possible below the line. The effective specific heat $\bar{c}_p$ is given by equation (61) and the dependence of $\bar{W}$ on $N_{Pr,i}$ and $N_{Sc,i}$ is given in figure 8 of reference 5. In practice a desirable ablation material would have a high value of $\bar{c}_p / c_{p,2}$ and the boiling temperature would not be reached.

When equation (74) is satisfied, equation (72) gives a limiting temperature $T_{i,max}$ above which the liquid temperature cannot be raised. Equating the right-hand side of equation (72) to zero (as $T_e - T_i$ becomes infinitely large) gives

$$\frac{1}{T_{i,max}} = \frac{1}{T_B} + \frac{R_1}{L_v} \log \left\{1 + \frac{M_1}{M_2} N_{Sc,i}^{-0.6} \left[\frac{\bar{c}_p}{c_{p,2}}\left(N_{Pr,i}^{0.6} - \frac{1}{3}\right) - \left(N_{Sc,i}^{0.6} - \frac{1}{3}\right)\right]\right\} \quad (75)$$

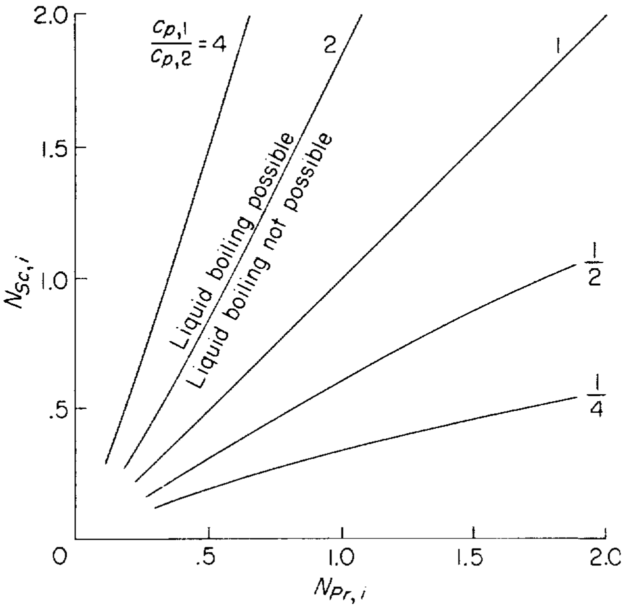

FIGURE 7.—Conditions under which boiling is possible.

This situation results from the shielding mechanism of the gas layer; each of the conditions (a), (b), and (c) tends to increase the shielding by the gas layer (as explained in detail in refs. 4 and 5) and, thus, restricts the amount of heat available for transfer across the gas-liquid interface. As the maximum temperature is approached and larger amounts of liquid are vaporized, any additional heat made available by increasing T_e is absorbed by the gas layer (since this layer must be heated in part to the high temperature T_e) which results only in additional convection of heat parallel to the gas-liquid interface without further increase in the heat transferred across the interface.

MASS-FLOW RATES

Asymptotic expressions for the rates of vaporization for large values of T_e-T_i are also easily

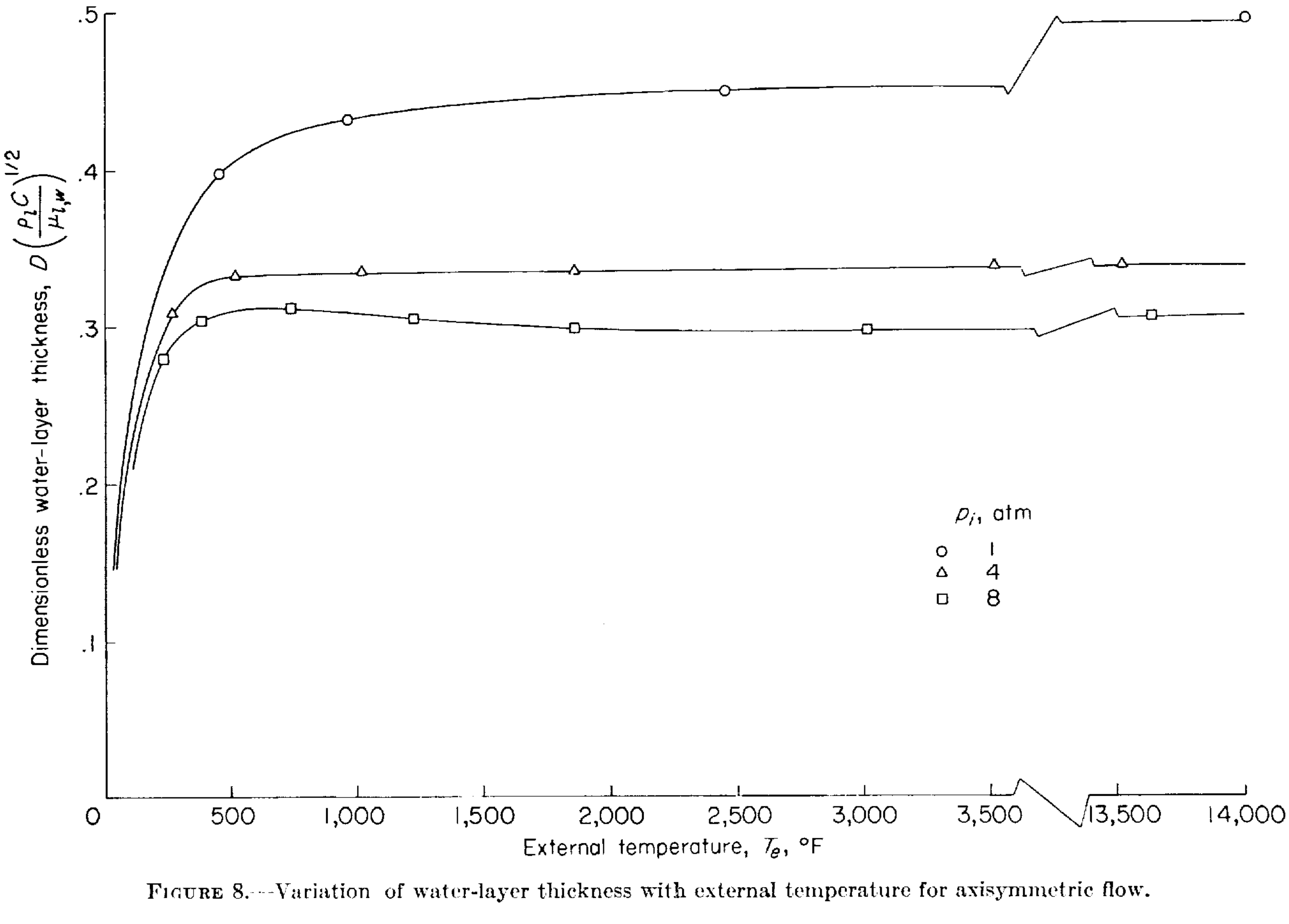

FIGURE 8.—Variation of water-layer thickness with external temperature for axisymmetric flow.

obtained from equation (59) as

$$\frac{\dot{m}_i}{(\rho_e\mu_e C)^{1/2}} \rightarrow \frac{\alpha_1 N_{Pr,i}{}^{-0.6}}{\frac{\overline{c}_p}{c_{p,2}}\left(1-\frac{1}{3}N_{Pr,i}{}^{-0.6}\right)} \tag{76}$$

which depends only upon the gaseous properties of the ablation material. Thus, a relation of the following form is expected for large values of T_e-T_i:

$$\frac{\left[\frac{\dot{m}_i}{(\rho_e\mu_e C)^{1/2}}\right]_{2-dim}}{\left[\frac{\dot{m}_i}{(\rho_e\mu_e C)^{1/2}}\right]_A}=\frac{(\alpha_1)_{2-dim}}{(\alpha_1)_A}=0.745 \tag{77}$$

For small values of T_e-T_i, where $\dot{m}_i$ is neglected, equation (59) reduces to

$$\frac{\dot{m}}{(\rho_e\mu_e C)^{1/2}}=\frac{\alpha_1 c_{p,2}(T_e-T_i)N_{Pr,i}{}^{-0.6}}{c_b(T_w-T_b)+L_m+\frac{2}{3}c_l(T_i-T_w)} \tag{78}$$

and therefore, again,

$$\frac{\left[\frac{\dot{m}}{(\rho_e\mu_e C)^{1/2}}\right]_{2-dim}}{\left[\frac{\dot{m}}{(\rho_e\mu_e C)^{1/2}}\right]_A}=\frac{(\alpha_1)_{2-dim}}{(\alpha_1)_A}=0.745 \tag{79}$$

since there is a single relation between T_e and T_i. The relations (77) and (79) can be expected to hold approximately in the entire range since they reflect the dependence of the mass-flow rates on the relevant heat-transfer coefficients.

LIQUID-LAYER THICKNESS

Since the relations (77) and (79) are approximately valid in the entire temperature range, they lead to a similar ratio between the values of the liquid-layer thickness. Equations (65), (78), and (79) give the following result:

$$\frac{\left[D\left(\frac{C\rho_l}{\mu_{l,i}}\right)^{1/2}\right]_A}{\left[D\left(\frac{C\rho_l}{\mu_{l,i}}\right)^{1/2}\right]_{2-dim}}=\frac{(\alpha_1)_{2-dim}}{(\alpha_1)_A}=0.745 \tag{80}$$

As a check, equation (62) with $\frac{\dot{m}_i}{(\rho_e\mu_e C)^{1/2}}=0$ gives

$$\frac{\left[D\left(\frac{C\rho_l}{\mu_{l,i}}\right)^{1/2}\right]_A}{\left[D\left(\frac{C\rho_l}{\mu_{l,i}}\right)^{1/2}\right]_{2-dim}}=\frac{\left[\left(\frac{\alpha_1}{\alpha_2}\right)^{1/2}\right]_A}{\left[\left(\frac{\alpha_1}{\alpha_2}\right)^{1/2}\right]_{2-dim}}=0.752$$

The variation of the liquid-layer thickness depends largely on the variation of viscosity $\mu_{l,i}$ with temperature and on the rate of vaporization. For low heating rates, when

$$\frac{\dot{m}_i}{(\rho_e\mu_e C)^{1/2}}<<\frac{\dot{m}}{(\rho_e\mu_e C)^{1/2}},$$

equation (62) shows that

$$D\left(\frac{C\rho_l}{\mu_{l,w}}\right)^{1/2}\propto\left[\frac{\dot{m}}{(\rho_e\mu_e C)^{1/2}}\frac{\mu_{l,i}}{\mu_{l,w}}\right]^{1/2}$$

For most liquids, however, the viscosity decreases as the temperature increases and this effect may be sufficient to cause D to decrease for part of the range of heat-transfer rates. When appreciable vaporization occurs, the interface shear stress imposed by the gas boundary layer is reduced (as evidenced by eqs. (41) and (42)); as a result the liquid layer adjusts itself by increasing the thickness until the interface stress $\mu_{l,i}\frac{u_{l,i}}{D}$ again balances that of the gas boundary layer. The detailed behavior of the liquid layer depends on the balance of these opposing effects—that is, the increase in the rate of liquid flow and the reduction in shear stress which tend to increase the thickness and the reduction in liquid viscosity which tends to decrease the thickness.

EFFECTIVE THERMAL CAPACITY

A measure of the effective thermal capacity of the ablation material is given by

$$H_{eff}=\frac{q_{i,0}}{\dot{m}}$$

where $q_{i,0}$ is the rate of heat transfer to a nonablating body at a surface temperature T_i; that is, from equations (21), (23a) (or (23b)), and (60b) (or (60c))

$$q_{i,0}=\alpha_1(\rho_e\mu_e C)^{1/2}c_{p,2}(T_e-T_i)N_{Pr,i}{}^{-0.6}$$

The parameter H_{eff} is herein defined as the total amount of heat absorbed by unit mass of the material in solid, liquid, and gaseous states and should be as large as possible; H_{eff} depends on T_e-T_i rather than on T_e-T_w although in practice $\frac{T_e-T_i}{T_e-T_w}\approx 1$.

Equation (59) may thus be written

$$q_{i,0}=[c_b(T_w-T_b)+L_m+\frac{2}{3}c_l(T_i-T_w)]\dot{m}+\left[\frac{1}{3}c_l(T_i-T_w)+L_v+(\bar{c}_p+Jc_{p,2})\left(1-\frac{1}{3}N_{Pr,i}{}^{-0.6}\right)(T_e-T_i)\right]\dot{m}_l \quad (81)$$

Equation (81) shows that in unit time an amount of heat $q_{i,0}$ causes a total mass loss $\dot{m}$ of which $\dot{m}_l$ is vaporized. The total mass loss $\dot{m}$ absorbs a quantity of heat $c_b(T_w-T_b)+L_m$ in the solid state and $\frac{2}{3}c_l(T_i-T_w)$ as a liquid—that is, the average temperature rise in the liquid layer is $\frac{2}{3}(T_i-T_w)$; the amount $\dot{m}_l$ is further raised through a temperature difference $\frac{1}{3}(T_i-T_w)$ to T_i and absorbs an amount of heat L_v during vaporization and an additional amount $(\bar{c}_p+Jc_{p,2})\left(1-\frac{1}{3}N_{Pr,i}{}^{-0.6}\right)(T_e-T_i)$ as a gas. The latter contribution is the gas-layer shielding and because of its dependence on T_e-T_i is usually the most important effect.

The effective heat capacity is then

$$H_{eff}=c_b(T_w-T_b)+L_m+\frac{2}{3}c_l(T_i-T_w)+\left[\frac{1}{3}c_l(T_i-T_w)+L_v+(\bar{c}_p+Jc_{p,2})\left(1-\frac{1}{3}N_{Pr,i}{}^{-0.6}\right)(T_e-T_i)\right]\frac{\dot{m}_l}{\dot{m}} \quad (82)$$

Equation (82) shows that H_{eff} increases rapidly with the rate of vaporization $\dot{m}_l$ since the dominant term is that which contains the factor T_e-T_i; thus, a liquid of low boiling temperature is desirable in order to make $\frac{\dot{m}_l}{\dot{m}}$ as near unity as possible.

APPLICATION TO A PARTICULAR EXAMPLE

The results of the analysis are now applied to the melting and vaporization of ice; the following numerical values were used in the solution of equations (59), (62), (65), and (66):

$T_b=-80°$ F
$T_w=32°$ F
$T_B=212°$ F ($p_i=1$ atm)
$T_B=290°$ F ($p_i=4$ atm)
$T_B=325°$ F ($p_i=8$ atm)
$c_b=0.5$ Btu/lb-°F
$c_l=1$ Btu/lb-°F
$L_m=144$ Btu/lb
$L_v=1070-0.5(T_i-32)$ Btu/lb
$N_{Pr,i}=0.7$
$N_{Sc,i}=0.5$
$M_1=18$
$M_2=29$

When these numerical values are used, $\bar{W}$ is found to be 0.925 and $\bar{c}_p/c_{p,2}$ is found to be 1.925; also,

$$\frac{N_{Sc,i}{}^{0.6}-\frac{1}{3}}{N_{Pr,i}{}^{0.6}-\frac{1}{3}}=0.69$$

Thus, the inequality of equation (74) is satisfied and boiling cannot occur; the limiting temperature at the gas-liquid interface is given by equation (75) as

$T_{i,max}=195°$ F ($p_i=1$ atm)
$T_{i,max}=265°$ F ($p_i=4$ atm)

and

$T_{i,max}=310°$ F ($p_i=8$ atm)

The relation between T_e and T_i was found to be the same for the axisymmetric and two-dimensional cases (with errors less than 1 percent in T_i) for each of the values of p_i. The ratios of dimensionless mass-loss rates and dimensionless liquid-layer thickness were approximately equal to 0.745 as suggested by equations (77), (79), and (80);

these ratios were always in the range from 0.737 to 0.757. In view of the relation between axisymmetric and two-dimensional results only the axisymmetric results are shown (figs. 8 to 12).

The variation of liquid-layer thickness is particularly interesting. As seen in figure 8, initially the dimensionless water-layer thickness $D\left(\frac{\rho_l C}{\mu_{l,w}}\right)^{1/2}$ increases rapidly with external temperature T_e and thereafter the thickness maintains an almost constant value, although the rate of liquid flow continues to increase (fig. 9).

For values of p_i less than 4 atmospheres the boiling point is low enough for the effects of vaporization and increasing mass flow to dominate that of the decreasing viscosity, and the water-layer thickness continues to increase slowly. At a value of p_i of 4 atmospheres these effects just balance and the thickness remains constant at 0.338 between 500° F and 14,000° F. At pressures greater than 4 atmospheres the boiling point is high enough for the decreasing viscosity to cause a local maximum before appreciable vaporization takes place; thereafter, the thickness decreases slightly and then slowly increases again as vaporization increases. For each of the three pressures considered the variation in water-layer thickness is small in the temperature range 1,000° F $<T_e<$14,000° F.

The dimensionless rate of vaporization is virtually independent of the interface pressure p_i as seen in figure 10. The total rate of mass loss, however, does vary with p_i; it decreases as p_i increases (fig. 9). This effect is due to the increase in interface temperature with p_i (fig. 11), which reduces the rate of heat transfer from the outside stream (proportional to T_e-T_i) and also increases the average temperature of the liquid $\frac{2}{3}(T_i-T_w)+T_w$. This increases the liquid shielding and reduces the heat available for melting.

In figure 12 the effective heat capacity is seen

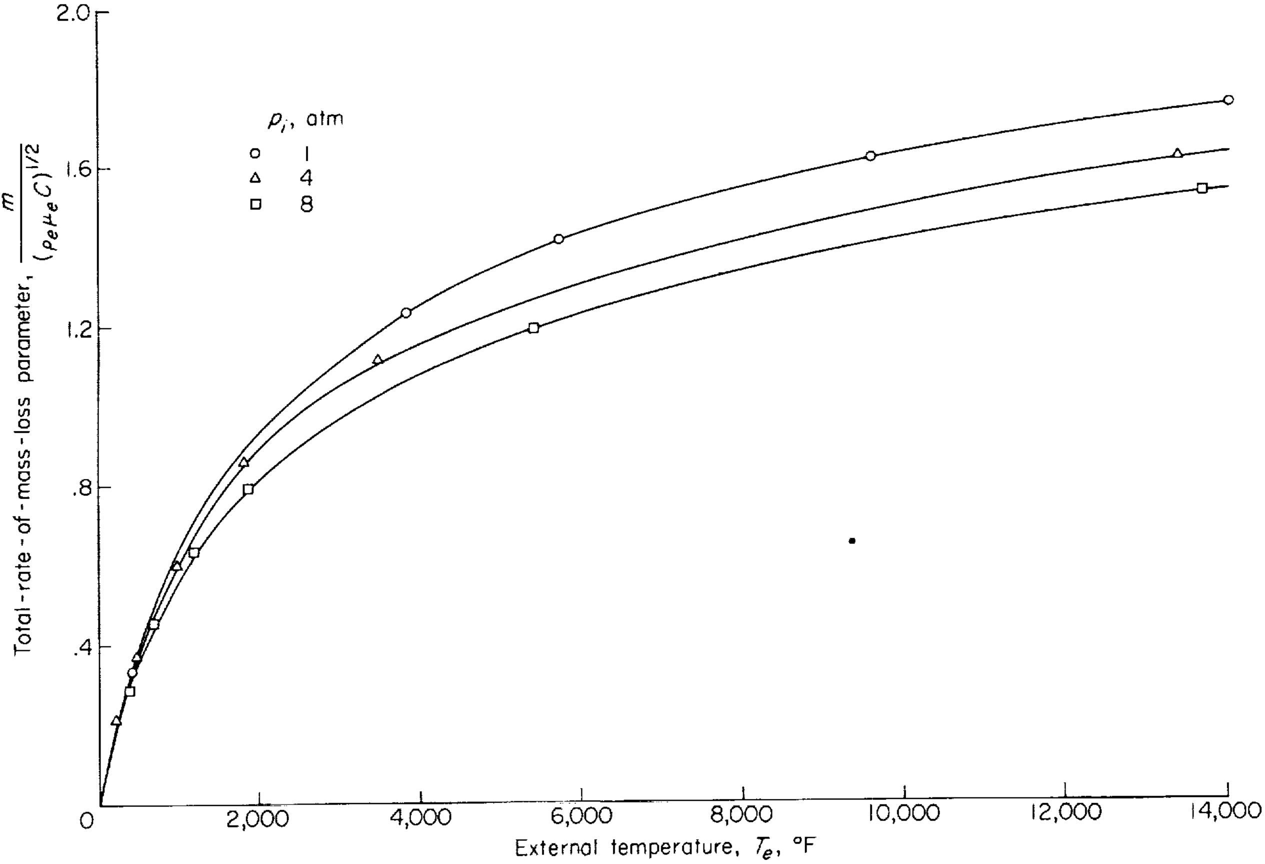

FIGURE 9. Variation of total-rate-of-mass-loss parameter with external temperature at various values of p_i for axisymmetric flow.

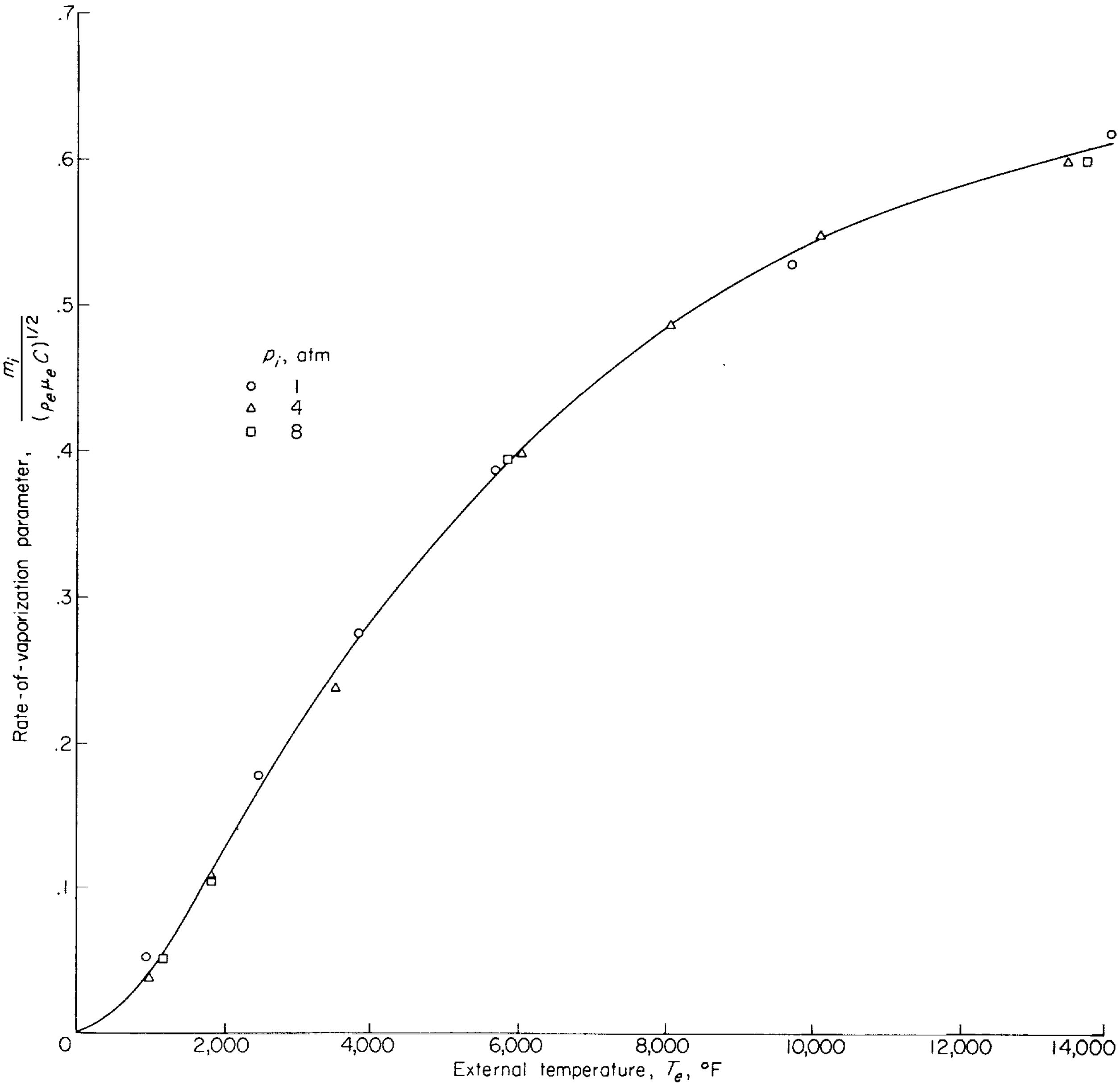

FIGURE 10.—Variation of rate-of-vaporization parameter with external temperature at various values of p_i for axisymmetric flow.

to increase with T_e and also with p_i; the latter effect is a result of the reduction in total mass loss. The greatest contribution to H_{eff} is made by the vapor, especially in the higher range of external temperatures where the shielding by the vapor layer increases while that due to the water layer is virtually constant and makes a maximum contribution of $\frac{2}{3} c_l(T_{i,max} - T_w)$ to H_{eff}.

CONCLUDING REMARKS

An approximate analysis has been made of steady melting and vaporization due to aerodynamic heating near the forward stagnation point of blunt bodies.

The shielding mechanism of the liquid and gas layers which form over the body is discussed qualitatively and quantitatively and numerical

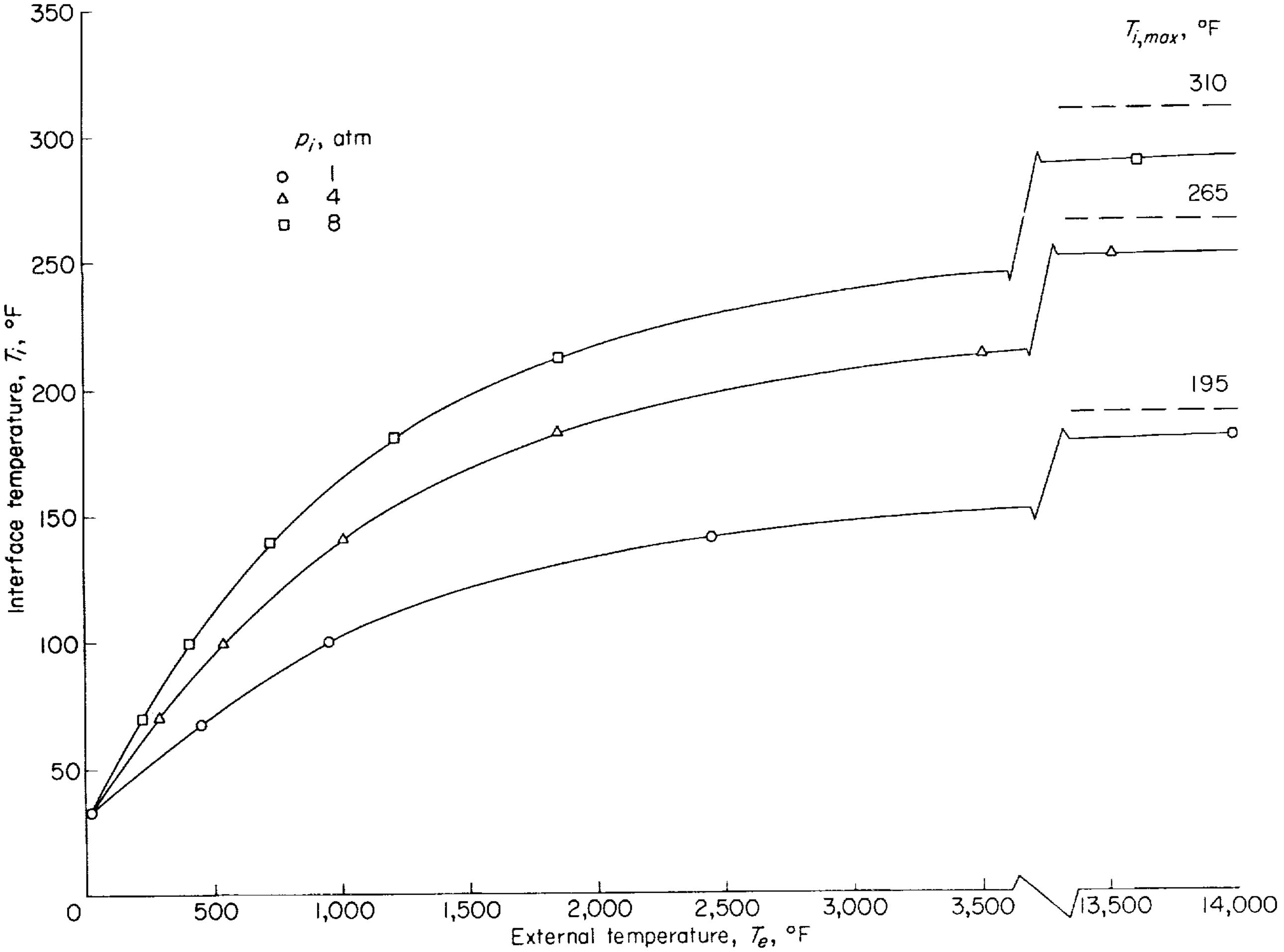

FIGURE 11.—Variation of interface temperature with external temperature at various values of p_i for axisymmetric flow.

results for a specific example, the melting and vaporization of ice, show that the greatest contribution to the shielding is made by the water-vapor layer when the heat-transfer rate is high enough.

It is shown that, for any material which melts, the liquid layer cannot attain the boiling temperature if the specific heat of the gas produced by vaporization has a high enough specific heat—that is, if the condition

$$\frac{\bar{c}_p}{c_{p,2}} > \frac{N_{Sc,i}^{0.6-\frac{1}{3}}}{N_{Pr,i}^{0.6-\frac{1}{3}}}$$

is satisfied ($\bar{c}_p$ is the mean effective specific heat of the gas mixture and the subscript i refers to the gas-liquid interface). In particular, when the Schmidt number N_{Sc} is equal to the Prandtl number N_{Pr}, this condition is satisfied if the specific heat of the gas produced $c_{p,1}$ is greater than that of air $c_{p,2}$. Thus, since $c_{p,1} > c_{p,2}$ is desirable in order to increase the gas-layer shielding, it is unlikely that the liquid layer will reach the boiling temperature when a desirable ablation material is used. A general conclusion is that shielding by the gas layer is much more effective than that of the liquid layer because of the large enthalpy difference across the gas layer.

The rate of ablation is shown to depend on the behavior of the liquid and gas layers and upon the interaction of these layers through the conditions relating rate of heat transfer and shear stress at their common interface. In particular, the effect

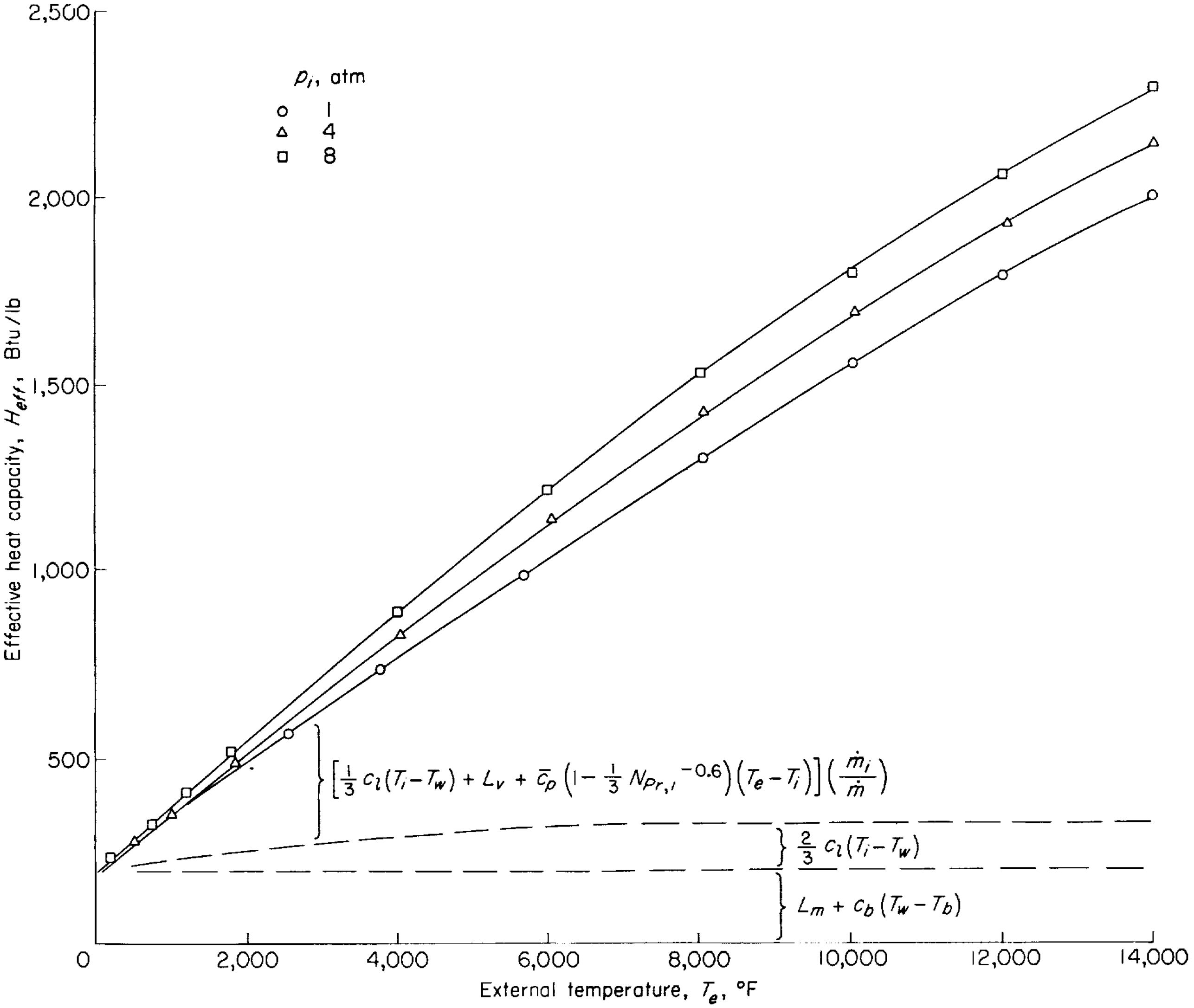

FIGURE 12.—Variation of effective heat capacity H_{eff} with external temperature T_e for axisymmetric flow.

of the rate of vaporization in reducing the interface shear stress has an important effect on the behavior of the liquid layer. The rate of melting of the solid and the reduction in interface shear stress cause the thickening of the liquid layer; the reduction in liquid viscosity, on the other hand, tends to reduce the layer thickness. These effects are displayed in the results for the example of melting ice.

LANGLEY RESEARCH CENTER,
NATIONAL AERONAUTICS AND SPACE ADMINISTRATION,
LANGLEY FIELD, VA., *November 18, 1958.*

REFERENCES

1. Roberts, Leonard: On the Melting of a Semi-Infinite Body of Ice Placed in a Hot Stream of Air. Jour. Fluid Mech., vol. 4, pt. 5, Sept. 1958, pp. 505–528.
2. Sutton, George W.: The Hydrodynamics and Heat Conduction of a Melting Surface. Jour. Aero. Sci., vol. 25, no. 1, Jan. 1958, pp. 29–32, 36.
3. Lees, Lester: Convective Heat Transfer With Mass Addition and Chemical Reactions. Presented at Third Combustion and Propulsion Colloquium of AGARD (Palermo, Sicily), Mar. 17–21, 1958.
4. Roberts, Leonard: A Theoretical Study of Stagnation-Point Ablation. NASA TR R-9, 1959. (Supersedes NACA TN 4392.)
5. Roberts, Leonard: Mass Transfer Cooling Near the Stagnation Point. NASA TR R-8, 1959. (Supersedes NACA TN 4391.)
6. Fay, J. A., and Riddell, F. R.: Theory of Stagnation Point Heat Transfer in Dissociated Air. Jour. Aero. Sci., vol. 25, no. 2, Feb. 1958, pp. 73–85, 121.
7. Beckwith, Ivan E.: Similar Solutions for the Compressible Boundary Layer on a Yawed Cylinder With Transpiration Cooling. NACA TN 4345, 1958.

U.S. GOVERNMENT PRINTING OFFICE: 1960